NASA/CR—2002-211899 ARL–CR–0509

NASA/DERA Collaborative Program—Interim Report

Phillip D. Whitefield and Donald E. Hagen
University of Missouri at Rolla, Rolla, Missouri

Jody C. Wormhoudt and Richard C. Miake-Lye
Aerodyne Research, Inc., Billerica, Massachusetts

Kevin Brundish and Christopher W. Wilson
Defence Evaluation and Research Agency, Farnborough, Hampshire, England

September 2002

The NASA STI Program Office . . . in Profile

Since its founding, NASA has been dedicated to the advancement of aeronautics and space science. The NASA Scientific and Technical Information (STI) Program Office plays a key part in helping NASA maintain this important role.

The NASA STI Program Office is operated by Langley Research Center, the Lead Center for NASA's scientific and technical information. The NASA STI Program Office provides access to the NASA STI Database, the largest collection of aeronautical and space science STI in the world. The Program Office is also NASA's institutional mechanism for disseminating the results of its research and development activities. These results are published by NASA in the NASA STI Report Series, which includes the following report types:

- TECHNICAL PUBLICATION. Reports of completed research or a major significant phase of research that present the results of NASA programs and include extensive data or theoretical analysis. Includes compilations of significant scientific and technical data and information deemed to be of continuing reference value. NASA's counterpart of peer-reviewed formal professional papers but has less stringent limitations on manuscript length and extent of graphic presentations.

- TECHNICAL MEMORANDUM. Scientific and technical findings that are preliminary or of specialized interest, e.g., quick release reports, working papers, and bibliographies that contain minimal annotation. Does not contain extensive analysis.

- CONTRACTOR REPORT. Scientific and technical findings by NASA-sponsored contractors and grantees.

- CONFERENCE PUBLICATION. Collected papers from scientific and technical conferences, symposia, seminars, or other meetings sponsored or cosponsored by NASA.

- SPECIAL PUBLICATION. Scientific, technical, or historical information from NASA programs, projects, and missions, often concerned with subjects having substantial public interest.

- TECHNICAL TRANSLATION. English-language translations of foreign scientific and technical material pertinent to NASA's mission.

Specialized services that complement the STI Program Office's diverse offerings include creating custom thesauri, building customized databases, organizing and publishing research results . . . even providing videos.

For more information about the NASA STI Program Office, see the following:

- Access the NASA STI Program Home Page at ***http://www.sti.nasa.gov***

- E-mail your question via the Internet to help@sti.nasa.gov

- Fax your question to the NASA Access Help Desk at 301–621–0134

- Telephone the NASA Access Help Desk at 301–621–0390

- Write to:
  NASA Access Help Desk
  NASA Center for AeroSpace Information
  7121 Standard Drive
  Hanover, MD 21076

NASA/CR—2002-211899 ARL–CR–0509

NASA/DERA Collaborative Program—Interim Report

Phillip D. Whitefield and Donald E. Hagen
University of Missouri at Rolla, Rolla, Missouri

Jody C. Wormhoudt and Richard C. Miake-Lye
Aerodyne Research, Inc., Billerica, Massachusetts

Kevin Brundish and Christopher W. Wilson
Defence Evaluation and Research Agency, Farnborough, Hampshire, England

Prepared under Contract NAS3–98102, and
Grants NAG3–2179 and NAG3–2185

National Aeronautics and
Space Administration

Glenn Research Center

September 2002

This report contains preliminary findings, subject to revision as analysis proceeds.

This Document was produced by QinetiQ for The Department of Trade and Industry
Under Order/Contract reference F11X1DXX

Available from

NASA Center for Aerospace Information
7121 Standard Drive
Hanover, MD 21076

National Technical Information Service
5285 Port Royal Road
Springfield, VA 22100

Available electronically at http://gltrs.grc.nasa.gov

Preface

The work performed herein was sponsored by NASA and by DERA, through the Department of Trade and Industry (DTI) Civil Aerospace Research and Development (CARAD) programme. The programme is managed by Dr. C. Wey (NASA) and Mr. K. Brundish (DERA).

The need to meet future emission legislation has been identified as a priority requirement for propulsion programmes worldwide. Sulphate aerosols and their precursors, such as SO_3, have been implicated in a number of significant physical and chemical processes in the upper atmosphere. These include persistent contrails and ozone depletion. Legislation restricting their emission may be tightened further as the understanding of these effects increases. The mechanisms of aerosol formation are themselves poorly understood, with limited data available for further investigation. This programme will characterise the emission of aerosols and aerosol precursors, including SO_2, SO_3 and HONO to further this understanding. This information will help understand if legislation is required. The programme of work aims to make a consistent set of data available for measurements at both the combustor exit and the engine exit. This will allow modelling to be performed to help understand the effects of the turbine and nozzle on the emissions.

This is an interim report covering the initial testing phase, that of the combustor exit plane emissions measurements. The work reported was performed at DERA Pyestock, UK, by the UK/U.S. collaborators.

Executive Summary

This report is an interim report produced for the DTI under CARAD programme F11X1DXX. The work reported are the results from the combustor testing, the first phase of testing in the DERA/NASA collaborative programme.

Aerosol emissions from aircraft engines are becoming of increasing concern due to their contribution to contrail formation. Cirrus cloud formation can increase by up to 25% within flight corridors. The consequences of this climate change effect are as yet unknown, although increased cloud coverage is known to contribute significantly to the greenhouse effect. Although much is still unknown about cloud formation, one mechanism is that aerosol emissions from the combustion process act as nucleation agents for the water vapour. Legislation restricting aerosol emissions may be introduced as the understanding of their effect increases.

The programme of work aims to make a consistent set of data available for measurements at both the combustor exit and the engine exit. This will allow modelling to be performed to help understand the effects of the turbine and nozzle on the emissions. The experimental work must be performed such that the combustor inlet conditions are identical for both the combustor testing and the engine testing. The emissions measurements must also be performed at realistic operating conditions for a typical gas turbine engine. In order to achieve this, special facilities are required with a large degree of control over both combustor and engine parameters.

The measurement of aerosols and aerosol precursors is difficult, with techniques still in development. Much of the early development for these measurement techniques was performed within the U.S. As such, a programme of work was developed by DERA and NASA utilising specialist facilities within the UK, and specialist measurement techniques developed within the U.S. Under a Memorandum of Understanding (MoU) between the UK and U.S. governments, the joint UK/U.S. funded programme commenced. The objective of the programme was to make combustor and engine exit plane emissions measurements, including particulate and sulphur measurements, for kerosene fuels with different sulphur levels. The emissions measurements will be utilised to develop and validate combustion models, with the ultimate aim of improving the prediction of aviation effects on the environment. The combustor exit plane emissions will be used as inlet boundary conditions for the modelling. The engine exit plane emissions will be used for validation for modelling the effect of the turbine on both particulate and sulphur chemistry.

The combustor test programme was performed in August/September 2000. Although probe issues complicated the test programme, a consistent set of data, including CO, NO_x, NO, NO_2, CO_2, O_2, smoke number, particulate number density and size distribution, SO_2, SO_3 and HONO were collected at the exit plane of the DERA TRACE engine combustor. A second probe was utilised to measure spatial location of CO, NO_x, NO, NO_2 and CO_2 concentrations. Data are therefore available for development of aerosol, particulate and aerosol precursor chemistry sub-models for inclusion into CFD. Inlet boundary conditions have been derived at the exit of the combustion system for the modelling of the DERA TRACE engine.

The second phase of the programme is to perform identical measurements at the engine exit, to allow a full data set to be available. This will be performed in July 2001 at the Glenn test facility, DERA Pyestock.

Table of Contents

1 Introduction

Aerosol emissions from aircraft engines are becoming of increasing concern due to their contribution to contrail formation. Cirrus cloud formation can increase by up to 25% within flight corridors **[1]**. The consequences of this climate change effect are as yet unknown, although increased cloud coverage is known to contribute significantly to the greenhouse effect. Although much is still unknown about cloud formation, one mechanism is that aerosol emissions from the combustion process act as nucleation agents for the water vapour. Legislation restricting aerosol emissions may be introduced as the understanding of their effect increases.

The need to meet future emission legislation has been identified as a priority requirement for propulsion programmes worldwide. Sulphate aerosols and their precursors, such as SO_3, have been implicated in a number of significant physical and chemical processes in the upper atmosphere. These include persistent contrails and ozone depletion. Legislation restricting their emission may be tightened further as the understanding of these effects increases. The mechanisms of aerosol formation are themselves poorly understood, with limited data available for further investigation. This programme will characterise the emission of aerosols and aerosol precursors, including SO_2, SO_3 and HONO to further this understanding. This information will help understand if legislation is required.

The programme of work aims to make a consistent set of data available for measurements at both the combustor exit and the engine exit. This will allow modelling to be performed to help understand the effects of the turbine and nozzle on the emissions. The experimental work must be performed such that the combustor inlet conditions are identical for both the combustor testing and the engine testing. The emissions measurements must also be performed at realistic operating conditions for a typical gas turbine engine. In order to achieve this, special facilities are required with a large degree of control over both combustor and engine parameters.

The measurement of aerosols and aerosol precursors is difficult, with techniques still in development. Much of the early development for these measurement techniques was performed within the U.S. As such, a programme of work was developed by DERA and NASA utilising specialist facilities within the UK, and specialist measurement techniques developed within the U.S. Under a Memorandum of Understanding (MoU) between the UK and U.S. governments, the joint UK/U.S. funded programme commenced. The objective of the programme was to make combustor and engine exit plane emissions measurements, including particulate and sulphur measurements, for kerosene fuels with different sulphur levels. The emissions measurements will be utilised to develop and validatecombustion models, with the ultimate aim of improving the prediction of aviation effects on the environment. The combustor exit plane emissions will be used as inlet boundary conditions for the modelling. The engine exit plane emissions will be used for validation for modelling the effect of the turbine on both particulate and sulphur chemistry.

The UK agreed to provide, through DTI funding to DERA, specialist test facilities, standard gas analysis, and gas turbine experience. The U.S. agreed to provide, through funding from NASA to Aerodyne and the University of Missouri Rolla, expertise in sulphur species and particulate emissions measurements, respectively.

This information will then be used to develop and validate improved chemical kinetic and Computational Fluid Dynamic (CFD) models, enhancing our ability to predict the composition and characteristics of particulate and aerosol emissions from aircraft engines. Massachusetts Institute of Technology and ARI will perform the modelling and validation work, also funded by NASA.

This report is an interim report, and describes the results from the combustor exit plane measurements.

2 DERA Test Facility and Probe Design

2.1 Test Facility

In order to achieve measurements in a controlled environment, the testing was performed on the DERA TRACE engine combustor. The TRACE engine is fitted with 10 tubo-annular combustors, Figure 1, which are representative of a CAEP 4 compliant engine. Although not fully representative of the annular combustors typical in modern engines, it allows excellent control of experiment design to ensure that testing of a single combustor in a rig will be representative of the combustor in the engine. In order to test annular combustion systems for research, sectors of the combustor are utilised to reduce testing costs. This introduces inaccuracies as side-walls are required, and there is concern that combustor rig testing is not representative of the combustor within the engine.

The DERA TRACE combustor was therefore used to obtain emissions measurements at the exit plane (Figure 2). The combustor, a single flame tube as shown in Figure 1, was tested on the Sector Combustor Rig (SCR) at DERA Pyestock (Figure 3). Separate control over temperature (up to 900K, non-vitiated), mass flow (up to 5 Kg/s) and pressure (up to 10 bar) is available, allowing a wide variation of combustor inlet conditions to be achieved. The rig arrangement allows 4 degrees of freedom (pitch, yaw, axial and rotational translation) and minimises the amount of bends required to extract the sample to the measurement systems due to it being inserted directly downstream of the combustor exit plane. This is beneficial to both sulphur and particulate emissions measurement techniques.

2.2 Probe Design

Wall reactions can account for enormous conversion of sulphur compounds before the gas sample reaches the measurement equipment if the probe design is insufficient. Similar problems also exist for particulate measurements, although not as severe, where the cold surface of the probe can result in particulate deposition to the wall. In addition to wall reaction issues, the probe was required to feed three measurement systems, that of DERA, UMR and Aerodyne. Sufficient flow to the three systems was desirable, such that the measurements could be performed simultaneously to reduce expensive facility running time.

To fulfill the above outlined requirements, a special probe was designed using Computational Fluid Dynamics (CFD) to ensure the sample had minimum contact with the probe surfaces. Figure 4 shows the probe design, with Figure 5 showing it installed in the SCR facility. The gas sample feed to the Aerodyne system for sulphur compound measurements was positioned to minimise surface contact of the gas flow. Figure 6 shows the flow regime within the probe, and shows the central streamtubes remaining free from contact with the probe walls. The resulting internal probe diameter was larger than for probes normally designed for gas extraction, in order to reduce the surface area/volume ratio. The small orifice at the entry to the Aerodyne feed allowed sub-atmospheric pressures to be achieved downstream, necessary for the Aerodyne measurement equipment. Downstream of the small orifice nitrogen purge was injected along the wall to continue to minimise gas flow surface contact. The UMR and DERA feeds were taken at an angle of approximately 45 degrees, minimising the disturbance on the flow and allowing the bulk of the flow to remain free of surface contact.

CFD was also utilised in the design of the cooling water system, required to ensure adequate probe survival in the harsh environment of the gas turbine combustor with exit gas temperatures of up to 2000K. In addition to probe survival, the cooling water must reduce the gas sample temperature sufficiently to quench reactions, although it is recognised that this is not possible for sulphur reactions, such that the sample arriving at the measurement systems is representative of the exit plane. This is particularly important in halting the chemistry of CO and NO_x, and as such the sample is quenched to 150 degrees C. The temperature of the sample cannot be lowered further without risk of water condensation that can remove oxides of nitrogen and sulphur by conversion into nitric and sulphuric acid.

The probe initially warped during testing, making it difficult to determine position, and finally failed. The failure is shown in Figure 7, a split in the probe, whilst Figure 8 shows the distortion which occurred during testing. As a consequence, the data obtained from the specialist sulphur probe could be used to examine relationships between species but could not be spatially resolved. A more standard probe (Figure 9), typically used on the SCR facility, was used to obtain a reference database that was spatially resolved.

Although in theory adequate life could be obtained with the cooling water flow rates and pressures utilised, the probe suffered a catastrophic failure during the test programme. In order to minimise probe outer diameter to reduce its effect on the internal combustor flowfield, and to maximise the internal diameter to improve the accuracy of the sulphur measurements the cooling water passages were minimised. Although these heights allowed sufficient cooling water flow for sustained life, when considered in conjunction with manufacturing tolerances the passage heights were marginal. It is thought that the marginal passage heights may have suffered a blockage during the testing, leading to non-uniform heating.

3 Test Programme

The baseline fuel utilised was a low sulphur fuel, with the specification outlined in Table 1. Many low sulphur fuels are hydra-treated, and the aromatic content is reduced to insignificant amounts (<0.5%). It is well known that low aromatic concentration affects particulate emissions. Therefore a fuel was used with an aromatic content of 15%, typical of current aviation fuels, to avoid the issue. The sulphur additive, DiMethyl DiSulphate (DMDS) was input (using a doping pump) into the fuel system about 2m upstream of the fuel injector, allowing adequate mixing before injection into the combustor. The goal was to examine several sulphur levels spanning a range of fuel sulphur contents: 30ppm, 300ppm and 3000ppm. The lower two sulphur levels represented the range of typical aviation fuels **[2]**, with the highest concentration representing the upper limit for aviation fuels. Although it is unlikely that aviation fuel would contain such high levels of sulphur (3000ppm), it exaggerates the effect on particulate and sulphur emissions. Although the doping pump was calibrated, its accuracy was limited, and thus some points with sulphur values outside the above stated levels were recorded. The sulphur levels were confirmed with separate fuel analysis by the Fuels and Lubrication Department, DERA Pyestock.

The running conditions for the combustor were set based on achieving the same actual conditions for the combustor in the ensuing engine tests. Cruise condition was examined as the main point of interest for the effect of the emissions (Table 3-2). However, initial modelling results from MIT/ARI had suggested it would be prudent to evaluate the sulphur chemistry at elevated temperatures compared to the cruise condition of the TRACE engine. The Glenn engine test facility at DERA Pyestock allows the control of engine parameters not normally available with standard engine control system. A model of the TRACE engine was utilised to determine the maximum combustor exit temperature that could be achieved whilst limiting the combustor inlet pressure to 10 bar, the upper limit of the SCR test facility. By adjusting the compressor inlet guide vanes, and adjusting the engine bleeds, the maximum combustor exit temperature achievable without engine stall or surge was derived, and is outlined in Table 2 (uprated cruise). Although this did not result in as high a combustor exit temperature as desired, it was considered more important to ensure that the inlet conditions for the combustor were identical in both the engine and combustor rig tests.

In summary, the following test matrix was performed:

uprated cruise condition with the following sulphur concentrations:
8ppm
550ppm
1600ppm
2350ppm
2500ppm
11650ppm

cruise condition, with the following sulphur concentrations:
8ppm
830ppm
2300ppm

Due to the problems of the specialist probe design, testing was also performed at uprated cruise condition with 8ppm sulphur concentration using a conventional probe. A complete listing of the sulphur levels is given in Table 3.

As part of the testing, a number of test facility operating parameters (as listed in Table 4) were recorded.

4 Emissions Measurement Systems

At each measurement location gas was extracted to a suite of emissions measurement equipment to characterise the DERA TRACE combustor. The measurement techniques utilised are outlined below. Detailed information pertaining to specific measurement equipment is supplied in the attached appendices. Each measurement was performed for a given spatial location on the exit plane.

DERA utilised commercially available gas analysis instrumentation to measure CO, CO_2, NO, NO_2, O_2 and smoke number (SAE). Details of the system configuration are given in Appendix A. All gas measurements were made in accordance with SAE Aerospace Recommended Practice ARP 1256 Rev B (Procedure for the continuous sampling and measurement of gaseous emissions from aircraft turbine engines). Smoke measurements were made in accordance with SAE Aerospace Recommended Practice ARP 1179 Rev B (Aircraft gas turbine engine exhaust smoke measurement) and ICAO Environmental Annex 16 volume 2. The data has been plotted against spatial location, in addition to plots against the local AFR.

The Cloud and Aerosol Sciences Laboratory at the University of Missouri-Rolla performed the following measurements on the particulate emissions as a function of the test matrix (described above):

- total particulate number density (TCN) at the source (i.e. in the combustor)
- number-based particulate size distributions for diameters ranging from 10nm to 1000nm (1μm).

A description of the experimental methodology underlying these measurements is given in Appendix B. Analysis of these measurements has provided a set of derived particulate emission parameters that include number- and mass-based emission indices and concentrations, and shape related parameters extracted from the size distributions.

Aerodyne Research Inc. performed infrared absorption measurements of gas sampled from the combustor, using infrared tuneable diode lasers and a multipass cell operating at reduced pressure. The apparatus used allows simultaneous measurements by two lasers operating in two separate spectral regions. However, to get both good spectral resolution and the fast scanning which suppresses noise, only one laser was operated at a time. One laser was devoted to measuring SO_x species, both the relatively stable SO_2 and the highly reactive SO_3. At different times, the SO_x laser was operated in two spectral regions to measure SO_2 and SO_3.

Another reactive species, HONO, was the target of the second laser diode. Here again, two spectral regions were used at almost every test point. Each of the spectral regions also contained absorption lines of water vapour, so that emission index values for SO_2, SO_3, and HONO can be derived directly from observations of concentrations of both the trace species and the water vapour. The use of multiple spectral regions was important in that it allowed estimation of the accuracy of SO_2, HONO and water concentration measurements directly from the observations. These measurements are discussed in greater detail in Appendix C.

5 Results and Discussion

A summary of the results is given below. A more detailed analysis of the data is reported in the individual Appendices, although as this is an interim report, full data analysis is not given.

5.1 Standard Gas Analysis Measurements

Measurements of exit plane CO, NO_x, NO, NO_2, CO_2, O_2 and smoke number emissions were performed for a range of different fuel sulphur contents on the DERA TRACE combustor. It was found that fuel sulphur level had no determinable effect on emissions of CO_2, NO_x, CO or smoke number. Consistent data sets were produced, although the specialist probe designed for sulphur measurements had insufficient life to complete the programme. A standard probe was therefore utilised to measure the above listed concentrations against spatial location. On comparison with the data collected using the larger diameter sulphur probe, it was found that different spatial patterns were exhibited for the emissions concentration data. This was thought to be due to a combination of a larger "sphere of influence" for the larger diameter probe drawing sample from a greater volume, and uncontrolled movement of the probe due to thermal warping. On comparison of the data for the two probes in a chemical domain, it was found that the larger probe suffered from continued reactions within the probe. Initial work has suggested that, for the species measured in the standard analysis package, only the measured concentration of CO emissions was affected by these continued reactions, although it is possible that SO_2 and HONO were also affected. This behaviour was modelled using a chemical kinetics package in order to determine a correction factor, although further work is still required.

5.2 Particulate Measurements

The particulate dependencies on fuel sulphur content and combustor operating conditions were explored. Little change was seen with sulphur level, and the conclusion was drawn that at the combustor exit plane, the sulphur content had no effect on particulate emissions.

The study of correlations between particulate parameters with gas phase species (measured by DERA) and engine operating conditions as probe position changed, did not yield anything of interest with the exception of those relating to SAE smoke number (see below). This would indicate that the range of physical and chemical mechanisms associated with the generation of the particulate parameters sampled at different points in the combustor exit plane are not systematically different to a degree that would allow such correlations to be observed.

SAE smoke number correlations were performed with the following particulate parameters; particulate mass, number-based particulate emission index (number of particulates per kilogram of fuel burned), mass-based particulate emission index (grams of particulate per kilogram of fuel burned where particulate assumed to be carbonaceous in composition, with spherical morphology and a uniform density of 1.5 g cm^{-3} (amorphous carbon)) and particulate surface area. Moderate correlations were observed between smoke number and particulate mass, number-based particulate emission index, and mass-based particulate emission index although

the best correlation was found to be between smoke number and particulate surface area. Theory would suggest this, as the particulate surface area should determine the light reflectance characteristics of the filter paper exposed to the aerosol during the smoke number measurement.

5.3 Aerosol Precursor Measurements

SO_3 concentrations were below the available detection limit, with best estimates to date being consistent with an upper limit on fraction of sulphur in the form of SO_3 in the combustor of, at most, a few percent. Comparison of measurements of SO_2 emission index with fuel analyses for total sulphur yield the same conclusion, that the great majority of sulphur was in the form of SO_2 in the combustor exhaust. Observed HONO concentrations were a small fraction of total NO_x emissions, although they may be large enough to raise the question of whether some HONO was formed in the sampling process.

In general, the TDL instrument operated well throughout the tests. Collection of data in multiple spectral regions proved to be a very useful diagnostic of measurement accuracy.

6 Conclusions

Although probe issues complicated the test programme, a consistent set of data, including CO, NO_x, NO, NO_2, CO_2, O_2, smoke number, particulate number density and size distribution, SO_2, SO_3 and HONO, were collected at the exit plane of the DERA TRACE engine combustor.

A second probe was utilised to measure spatial location of CO, NO_x, NO, NO_2 and CO_2 concentrations.

Data is therefore available for development of aerosol, particulate and aerosol precursor chemistry sub-models for inclusion into CFD.

Inlet boundary conditions have been derived at the exit of the combustion system for the modelling of the DERA TRACE engine.

7 Recommendations

The second phase of the programme is to perform identical measurements at the engine exit, to allow a full data set to be available. This will be performed in July 2001 at the Glenn test facility, DERA Pyestock.

8 References

1. Aviation and the Global Atmosphere, Edited by Joyce Palmer, David Lister, David Griggs, David Dokken and Mack McFarland, ISBN 0 521 66404 7, 1999.
2. The quality of aviation fuel available in the United Kingdom Annual Survey 1998, G.K. Rickard and J. Amero, DERA/MSS/MSMA/TR990400 August 1999

9 Tables

Name	Minimum	Maximum	Typical	Method
Density @ 15 °C	0.780	0.820		ASTM D1298
Distillation °C				ASTM D86
10% @	165	201	192	
F.B. Pt.	240	285	260	
Acidity mg KOH/gm		0.015	0.007	ASTM D3242
Aromatics %v/v	15.0	20.0	17	ASTM D1319
Doctor Test	Negative		Negative	ASTM D235
Freeze point °C		–47	< –47	ASTM D2386
Viscosity cS @ –20%	4.0	6.5	5.1	ASTM D445
Copper Corrosion		1	1	ASTM D130
Hydrogen Content %w/w	13.5	14.0	13.9	ASTM D3343
Total Sulphur %w/w		0.3	<0.01	ASMT D1266
Naphthalenes %v/v	1.0	3.0	2.3	ASTM D1840
Existent Gum mg/100ml		7.0	1	ASTM D381
W.I.S.M.	85		95	ASTM D3948
Conductivity pS/m	50	450	100	ASTM D2624
J.F.T.O.T. @ 260 °C				ASTM D3241
Tube Rating Visual		2.9	1	
or T.D.R. Spun		15		
Pressure Drop mm Hg		25	0	
Specific Energy MJ/Kg	42.86	43.5	42.9	IP 12
Smoke Point mm	20	28	25	IP 57
Abel Flash °C	38			IP 170
Silver Corrosion		1	1	IP 227

Table 1 – Fuel Specification

Combustor Inlet Conditions, Uprated Cruise:
Temperature 588K
AFR 56
Pressure 7.99Bar
Mass Flow 2.29Kg/s

Combustor Inlet Conditions, Standard Cruise:
Temperature 566K
AFR 66
Pressure 7.05Bar
Mass Flow 2.12Kg/s

Table 2 – Combustor Inlet Conditions

Date	Time	Condition	Sample Number	Pump Rate Hz	Result /ppm	Location
8/8/00	08:30	N/A	1 *	N/A	<7	Tanker
8/8/00	12:00		2		14 + full	BTH Tank
10/8/00	16:45	Shakedown	3*		<7	Rig
10/8/00	18:30	Shakedown	4		8	Rig
16/8/00	12:30	Run- S217C1T1 - no doping	5		37 + full	Rig
22/8/00	10:10	Uprated Cruise S220-C1T1	6	52	11650	Rig
22/8/00	10:30	Uprated Cruise S220 C1T1	7	30	1600	Rig
22/8/00	10:58	Cruise S220 C1T1	8	28.5	2300	Rig
22/8/00	14:05	Cruise S220 C1T2	9	24	830	Rig
22/8/00	16:45	Uprated Cruise S220 C1T3	10	38.5	2350	Rig
25/8/00	11:30	Uprated Cruise S221 C1T2	11	52	7500	Rig
25/8/00	12:15	Uprated Cruise S221 C1T3	12	24	550	Rig
25/8/00	15:30	Uprated Cruise S221 C1T3	13	24	400	Rig
31/8/00	10:03	Uprated Cruise S223 C1T1	14	24	340	Rig
31/8/00		*Uprated Cruise*	*15*	*24*	*430*	*Rig*
31/8/00	14:45 to 16:15 (90 min sample)	Uprated Cruise S223 C1T2	16	24	310	Rig

*Sulphur Detection limit for is 7 ppm

Table 3 – List of Sulphur Levels for Test Programme

Swirl meter air flow
Swirl meter signal
Swirl meter pressure
Swirl meter temperature
Main Orifice air flow
Main Orifice pressure
Main Orifice diff. pressure
Main Orifice temperature
Inlet pressure
Outlet pressure
Inlet temperature
Outlet temperatures
M root T/P
AFR
Fuel temperature
Main total fuel flow
Main 1 fuel flow
Main 1 fuel pressure
Box 1 Fuel pressure
Fuel pump delivery pressure
Wedge meter flow
Wedge meter P total
Wedge meter P diff
Wedge meter temperature
Traverser CW temp. in
Traverser CW temp. out

All instrumentation has full audit and calibration certification that is available on request.

Table 4 – List of Logged Rig Inlet Parameters

10 Figures

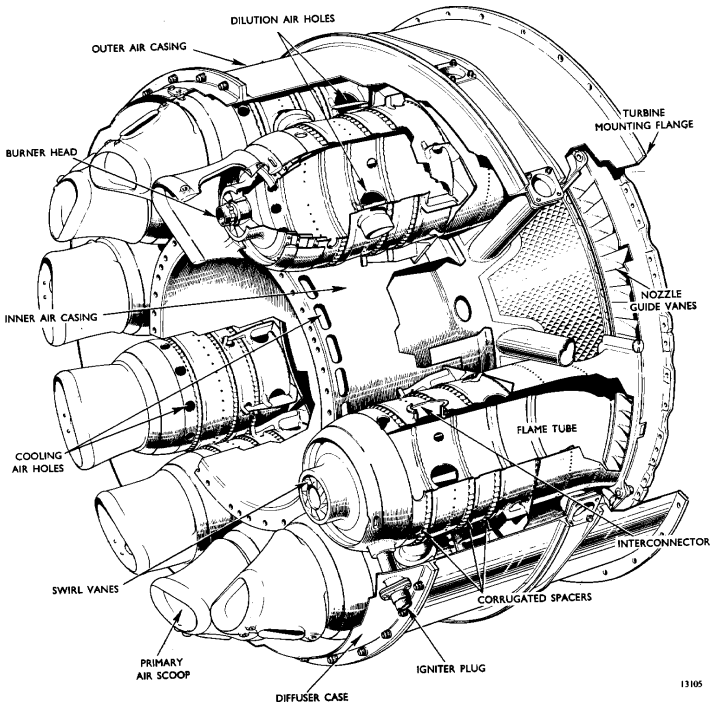

Figure 1 – DERA TRACE Engine

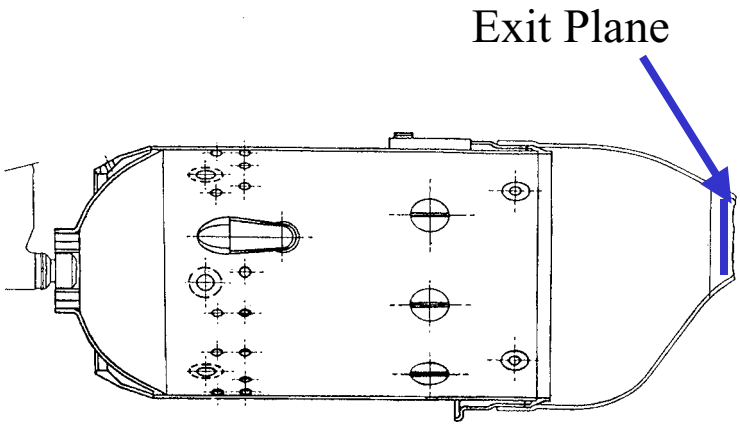

Figure 2 – DERA TRACE Combustor

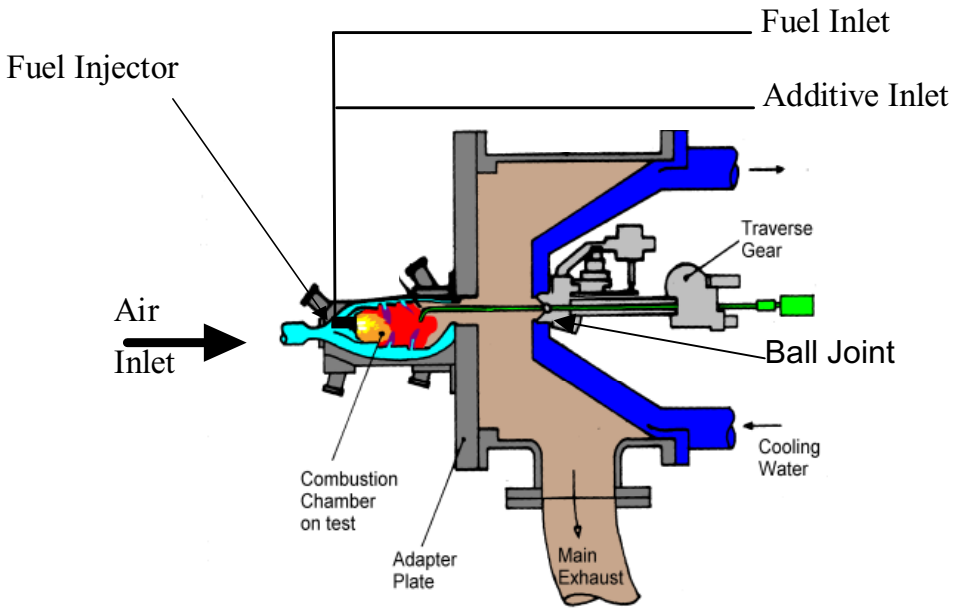

Figure 3 – SCR Test Rig

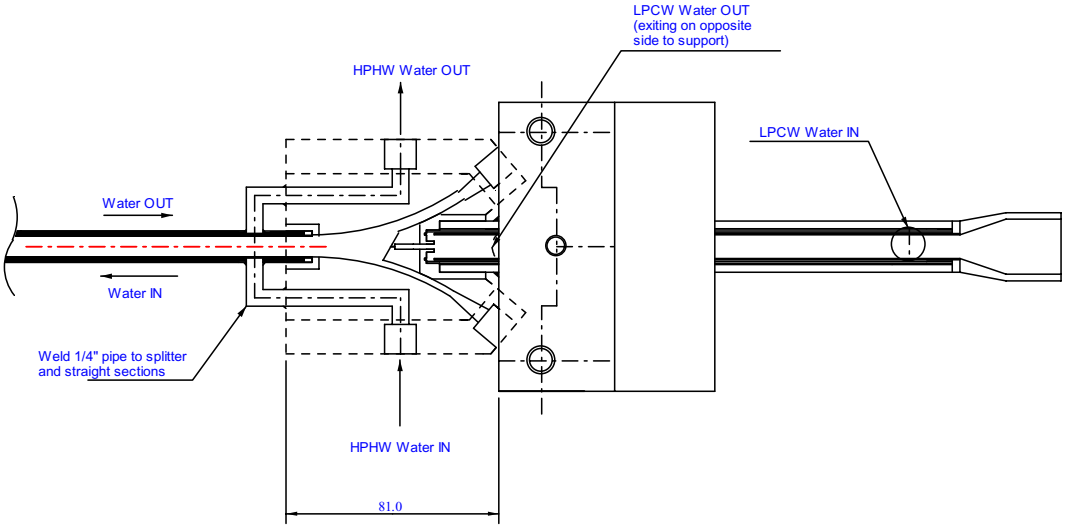

Figure 4 – Specialist Sulphur Probe

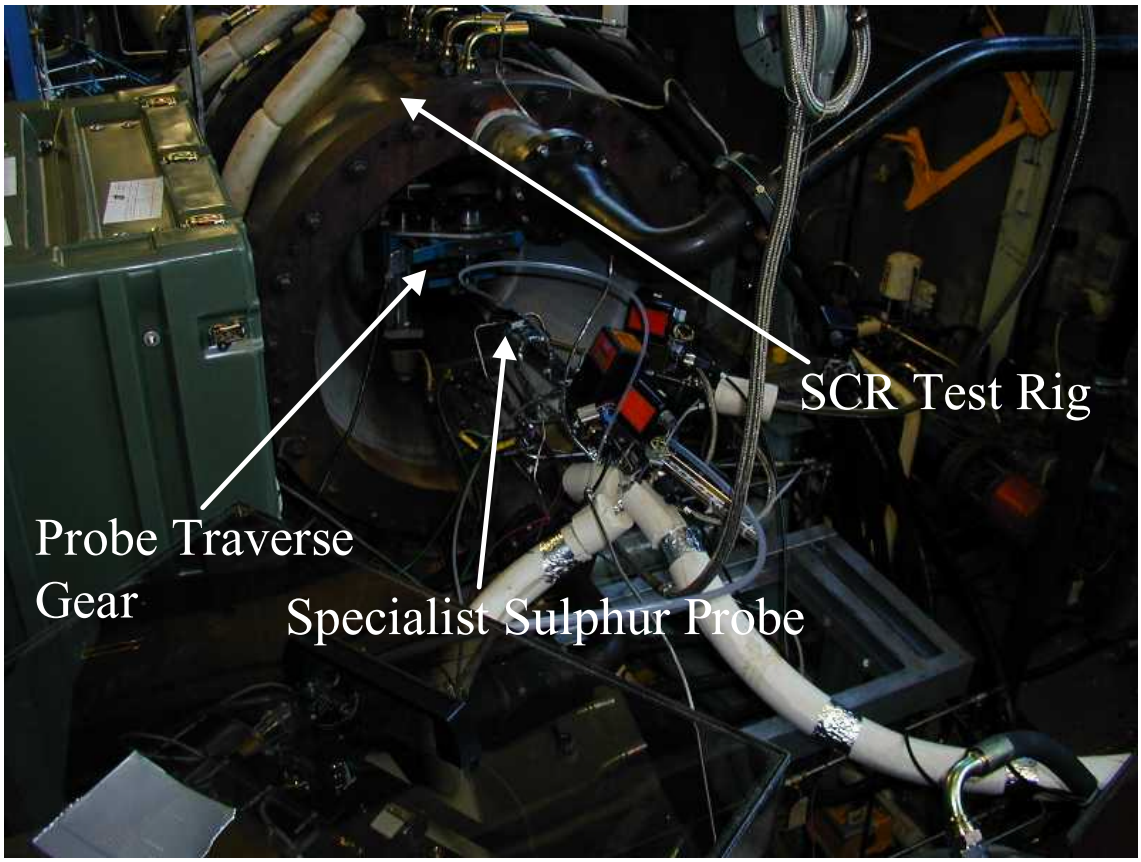

Figure 5 – Probe and Rig Assembly

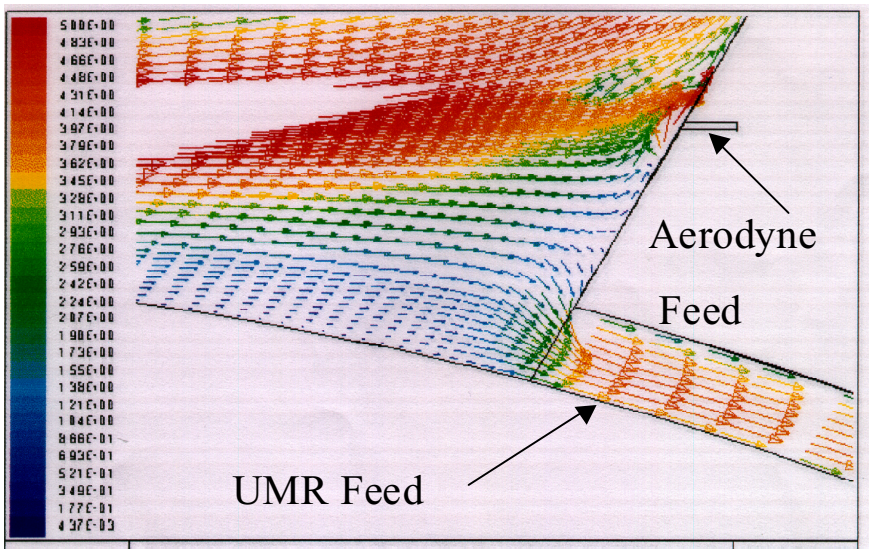

Figure 6 – Flow Regime within Probe

Figure 7 – Specialist Sulphur Probe Split

Figure 8 – Specialist Sulphur Probe Deformation/Warping

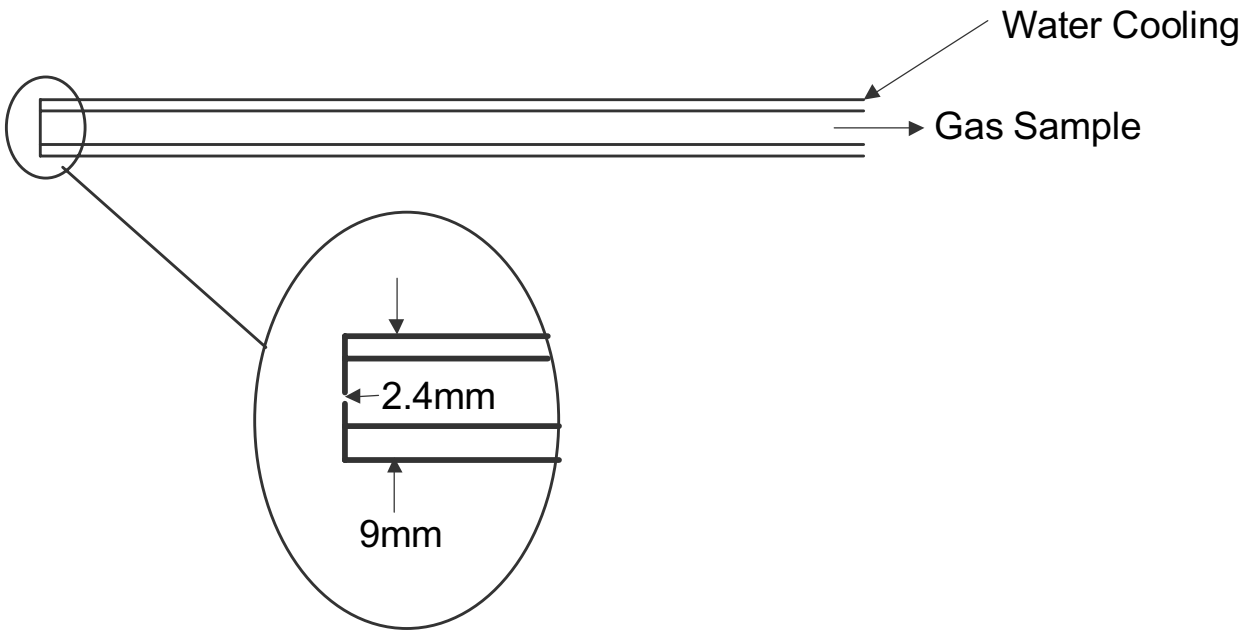

Figure 9 – Standard Probe

A Appendix—DERA Emissions Measurements

Kevin D. Brundish, Andrew R. Clague and Chris W. Wilson
Combustion and Environment Group
Defence and Evaluation Research Agency (Pyestock)
Farnborough, Hampshire, GU14 0LS

A.1 Experimental Configuration

As part of the DERA/NASA joint programme, DERA performed combustor exit plane emissions measurements of CO, CO_2, NO, NO_2, O_2. A schematic of the gas sampling equipment is shown in Figure 1. A list of the instrumentation utilised, is outlined in Table 1. A heated stainless steel sample line connected to the sample probe (as previously described) is used to convey the sample from the combustor to the gas analysis system. This sample acquisition system incorporates high pressure back purge air, which can be maintained at a pressure of 1500 Pa. This air is used to stop fuel flowing down the sample line at light-up, and also to clear the sample probe should it become blocked with soot (only usually required when internally traversing in the primary zone). The sample line, when flooded with fuel, behaves like a chromatographic column, in that the different fractions of fuel elute at different times. This can produce erroneous hydrocarbon measurements when sampling and therefore must therefore be avoided.

The sample probe orifice is very small and designed so that the sample enters at a high velocity and is quenched as it enters the relatively cool environment. It is important that condensation does not take place at any point in the system as species of interest may be lost on the walls of the sample line.

At a short distance from the DERA take off point the sample line is split into two separate channels. One of the sample lines leads to the smoke analysis equipment, which consists of both a filter stain, and an optical measuring technique. The other sample line conveys the sample to a filter oven to remove any particulate matter and then to the gas analysis suite. The gas analysers are used to measure carbon dioxide, carbon monoxide, hydrogen, total hydrocarbons, oxygen, nitrogen monoxide and oxides of nitrogen and smoke.

The NO/NO_x analyser, and the total hydrocarbon analyser measure the species concentration using a wet sample, whilst for the rest of the analysers the sample is dried. The dew point of the inlet air is measured so as to determine the concentration of ambient water. The dried sample dew point is also measured so that volume corrections may be applied. The NO/NO_x analyser is a dual channel system and so both species may be measured simultaneously.

The gas sampling systems ensures all gas measurements are made in accordance with SAE Aerospace Recommended Practice ARP 1256 Rev B (Procedure for the continuous sampling and measurement of gaseous emissions from aircraft turbine engines). Smoke measurements are made in accordance with SAE Aerospace Recommended Practice ARP 1179 Rev B (Aircraft gas turbine engine exhaust smoke measurement) and ICAO Environmental Annex 16

volume 2. The raw data is post processed as part of the recommended practices. This includes corrections for inlet air humidity, cross interference effects and dried sample corrections. All concentrations included within this report are corrected (denoted by c). The post processing also includes calculations of AFR, combustion efficiency and gas temperature.

A.2 Results and Discussion

A.2.1 Specialist Sulphur Probe Measurements

The DERA emissions measurements are presented in a number of formats. Figures 2 to 7 show the emissions concentrations plotted against AFR for the specialist sulphur probe. The c in the species concentration heading stands for corrected. On examining Figures 2 and 3, it can be seen that no discernible difference in CO_2 or NO_x concentration is evident for the different sulphur level fuels. The trends of increased NO_x and CO_2 as the AFR becomes richer provide evidence that a consistent data set was measured regardless of spatial location. Figure 2 also illustrates that NO_x increases for the uprated condition compared to the standard cruise condition. The higher inlet temperatures and pressures all give rise to higher flame temperatures, and hence higher NO_x emissions result.

Figures 4 and 5 show that over the range of AFRs measured, although some scatter exists, HC and CO values are low, with the resulting high combustion efficiency being independent of fuel sulphur level (Figure 6).

Smoke number against AFR is also included (Figure 7). The scatter of data for a given fuel sulphur level is larger than that for different sulphur levels. As a result, no trend can be established between fuel sulphur level and smoke number without a more detailed statistical analysis.

The complete data set, along with run number identifiers, can be found in Table 2. The table includes emissions concentrations and EI values, non-dimensioned to fuel flow (EI = g of pollutant/Kg of fuel). Inlet humidity data is also included. The column labelled SN refers to the SAE Smoke Number.

Figure 8 shows CO_2 levels against spatial location. The peak in CO_2 near the centre of the exit smile is expected in a single combustor such as the DERA TRACE combustor. However, the rich segment of the fuel injector (high CO_2) is large when considering that the fuel injector centreline is below that of the exit smile centreline. It was expected for this combustor that compression of the flow field as it passes through the smile would result in smaller peaks, located further outboard (above the centreline).

A.2.2 Comparison with Standard Probe Measurements

Figures 9 to 17 show the spatial location of the emissions measurements taken by the standard probe. When comparing Figure 8 and Figure 9 it is clear that the patterns in CO_2 are completely different. This was, initially, attributed to movement due to probe warping. However, it may also be caused the larger internal diameter of the specialist sulphur probe. The larger diameter probe would have a greater “sphere of influence” within the combustor, attracting sample from larger volumes within the combustor than the standard probe. Thus when centrally located, the larger diameter probe would extract sample from the uppermost regions, where high CO_2 values exist (Figure 9), thus making the CO_2 level artificially high. In an attempt to prove this

possibility, a number of values were extracted from the standard probe data set, averaged, and re-plotted. The pattern exhibited in Figure 8 could not be re-created, suggesting that internal probe diameter was not the sole reason for the different patterns. It is now thought that a combination of movement due to thermal warping of the probe and the larger internal diameter is the reason for the different patterns.

To ensure that the data set measured by the larger probe was of sufficient quality, the standard probe data, represented by the run number 224, were plotted against AFR along with the specialist sulphur probe data. Figures 18 and 19 show that the data sets are consistent when considering CO_2 and NOx. However, Figure 20 shows a reduced efficiency with the smaller diameter standard probe. On further examination, Figure 21 shows increased CO values with the smaller diameter standard probe. This variation is represented by the two diverging lines in Figure 21, which represent CO measurements for each of the two probes. One explanation for the differences is continued reactions in the larger diameter probe. The increased volume/surface ratio for the larger diameter probe would result in reduced cooling of the overall sample, and a high thermal gradient across the diameter. Consequently, continued combustion reactions may occur, reducing CO and increasing efficiency compared to the smaller diameter standard probe. With this possibility, a chemical kinetics (Chemkin) model was initiated for kerosene combustion within the probe. The modelling proved that reduced CO and comparable NO_x could be achieved due to different gas temperatures. Further investigation, using a quenching factor and the large probe data, showed that the Chemkin model could predict both the absolute values and the trends for standard probe data. Thus differential quenching for the probes was considered as the reason for the different CO and efficiency values, and work using Chemkin is being performed to derive a correction factor.

Density averaging of the results was also performed. The following procedure is used to obtain the density averaged results:

Calculate static temperature (T_s) at each point i on grid: $$T_s = T_t \left(\frac{p_t}{p_s} \right)^{\frac{\gamma-1}{\gamma}}$$

T_t = Total temperature K
p_t = Total pressure kPa (abs)
p_s = Static pressure kPa (abs).

In the absence of a shock system this can be taken as ambient pressure. γ, the ratio of specific heats, (C_p/C_v) is 1.4 for air, but 1.363 for engine exhaust at the conditions of the test. (Taken from on AGARD Properties of Air and Combustion Products with Kerosine & Hydrogen Fuels, 1967)

$$\text{Thus } \frac{(\gamma - 1)}{\gamma} = 0.2663$$

The average static temperature is given by:

$$T_{Smean} = \frac{n}{\Sigma\left(\frac{1}{t_s}\right)}$$

Calculate dynamic pressure (p_d) at each point i on grid: $p_d = p_t - p_s$

Calculate Mach No (Mi) at each point i on grid: $Mi = \sqrt{\frac{\left(\frac{p_t}{p_s}\right)^{\frac{\gamma-1}{\gamma}} - 1}{\frac{\gamma-1}{2}}}$

Each cell in the grid has a x-sectional area of dA = dx * dy = 50^2

Volume of exhaust gas passing through a cell per unit time = Vi * dA

where Vi = velocity in cell i = $\mathrm{Mi} \times \sqrt{\gamma \times \mathrm{R} \times \mathrm{t_s}}$ and R = 288

Except where there is a shock system this velocity should be similar to that calculated using the Bernoulli equation.

$$Vi = \sqrt{\frac{2 \times p_d}{density}}$$

Volume at STP of exhaust gas passing through a cell per unit time:

$$\mathrm{Vol}_i = \mathrm{V}_i . dA \left(\frac{273.15\,\mathrm{K}}{\mathrm{T_s}} \right) \left(\frac{\mathrm{p_s}}{101.325\,\mathrm{kPa}} \right)$$

Summing for all cells, givestotal volume at STP of exhaust gas per unit time:

$$\sum \mathrm{Vol} = \sum \left\{ \mathrm{Vi}.dA \left(\frac{273.15\,\mathrm{K}}{\mathrm{T_s}} \right) \left(\frac{\mathrm{p_s}}{101.325\,\mathrm{kPa}} \right) \right\}$$

Moles of species M per cell per unit time:

$$M_i = [M_0] \left(\frac{273.15\,\mathrm{K}}{\mathrm{T_s}} \right) \left(\frac{\mathrm{p_s}}{101.325\,\mathrm{kPa}} \right) \left(\frac{\mathrm{Vi}.dA}{22414\,\mathrm{cm}^3} \right)$$

where $[M_0]$ = mole fraction of species M at STP

Total moles of species M per unit time:

$$\sum Mol = \sum \left\{ [M_0] \left(\frac{273.15\,\mathrm{K}}{\mathrm{T_s}} \right) \left(\frac{\mathrm{p_s}}{101.325\,\mathrm{kPa}} \right) \left(\frac{\mathrm{Vi}.dA}{22414\,\mathrm{cm}^3} \right) \right\}$$

$$\text{Moles of species M per unit volume at STP} = \frac{\sum \text{Mol}}{\sum \text{Vol}}$$

$$\text{Average mole fraction of M: } [\mathrm{M_A}] = \frac{\sum Mol}{\sum Vol} \times 22414\ \mathrm{cm^3}$$

$$\text{Average g of M per unit volume: } \text{Mwv} = \text{MWt}\frac{\sum \text{Mol}}{\sum \text{Vol}}$$

$$\text{Average moles C per unit volume} = \frac{\sum \text{Mol CO}_2 + \sum \text{Mol CO} + \sum \text{Mol HC}}{\sum \text{Vol}}$$

Average kg Fuel per unit volume:

$$\text{Fwv} = \frac{(\sum \text{Mol CO}_2 + \sum \text{Mol CO} + \sum \text{Mol HC})0.012011}{\sum \text{Vol}}$$

$$\text{Average EI: } \text{EI}_A = \text{MWt}\frac{\sum \text{Mol}}{\sum \text{Volv}}\text{Fwv}$$

The density-averaged results are included in Table 3. This shows that, with the exception of CO, the results for the two probes were within experimental error, and confirms that a consistent data set was obtained using the specialist sulphur probe. Equilibrium modelling data is also included for CO_2 and temperature (Gordon/McBride). This also shows good agreement with the density-averaged data, again confirming the quality of the measurements.

A.3 Summary

In summary:

- Measurements of exit plane CO, NO_x, NO, NO_2, CO_2, O_2 and smoke number emissions were performed for a range of different fuel sulphur contents on the DERA TRACE combustor.
- Fuel sulphur level had no determinable effect on emissions of CO_2, NO_x, CO or smoke number.
- Consistent data sets were produced, although the specialist probe designed for sulphur measurements had insufficient life to complete the programme. Warping due to overheating led to difficulty in spatially resolving the data, before a catastrophic failure occurred.
- A standard probe was utilised to measure the above listed concentrations. On comparison with the data collected using the larger diameter sulphur probe, it was found that different spatial patterns were exhibited for the emissions concentration data. This was due to a combination of a larger “sphere of influence” for the larger diameter probe, and uncontrolled movement of the probe due to thermal warping.
- On comparison of the data for the two probes in a chemical domain, it was found that the larger probe suffered from continued reactions involving CO within the probe. This was modelled using Chemkin, in order to determine a correction factor.

A.4 Tables and Figures

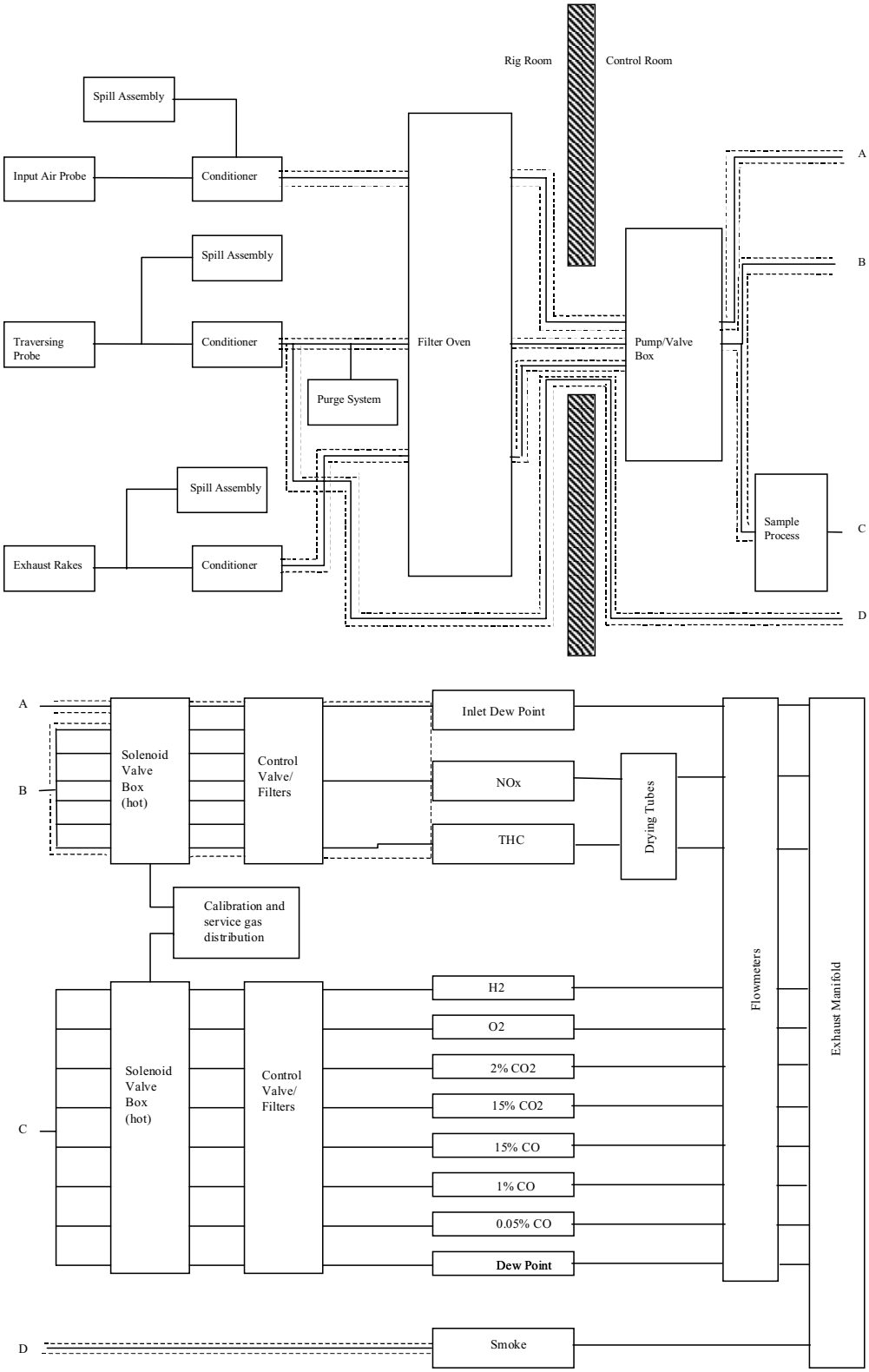

Figure 1 – Gas Analysis Schematic Diagram

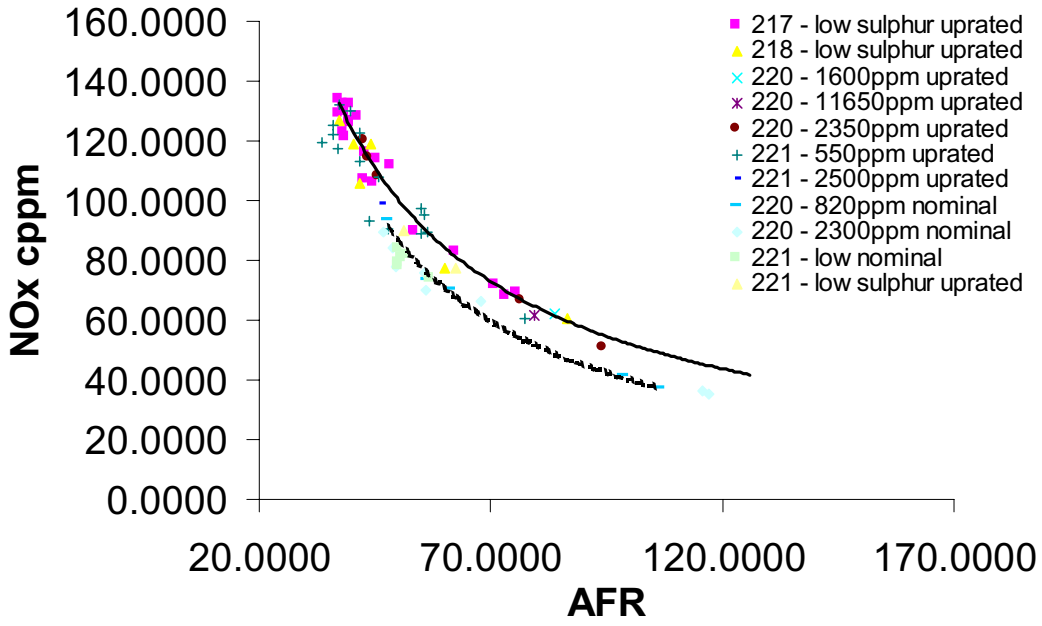

Figure 2 – NO_x vs AFR for all sulphur levels

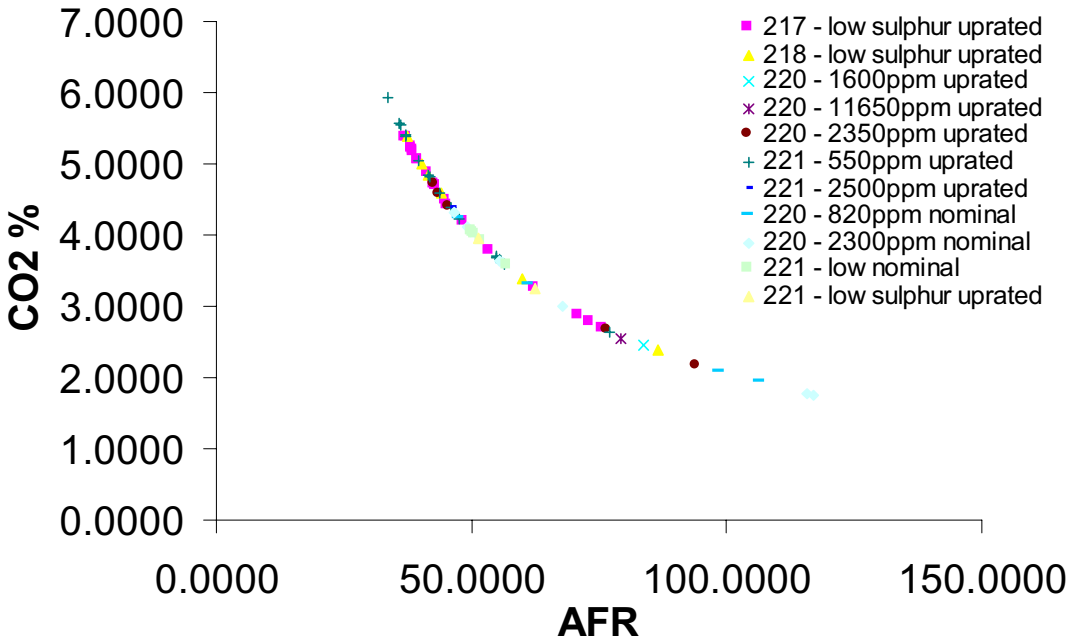

Figure 3 – CO_2 vs AFR for all sulphur levels

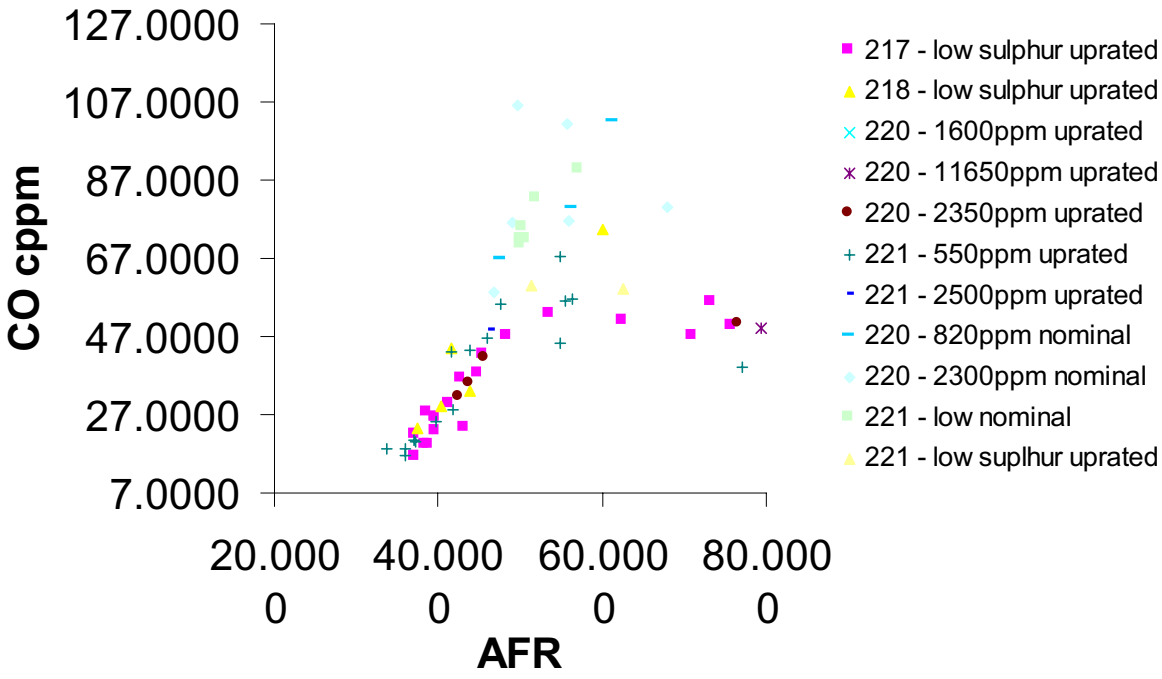

Figure 4 – CO vs AFR for all sulphur levels

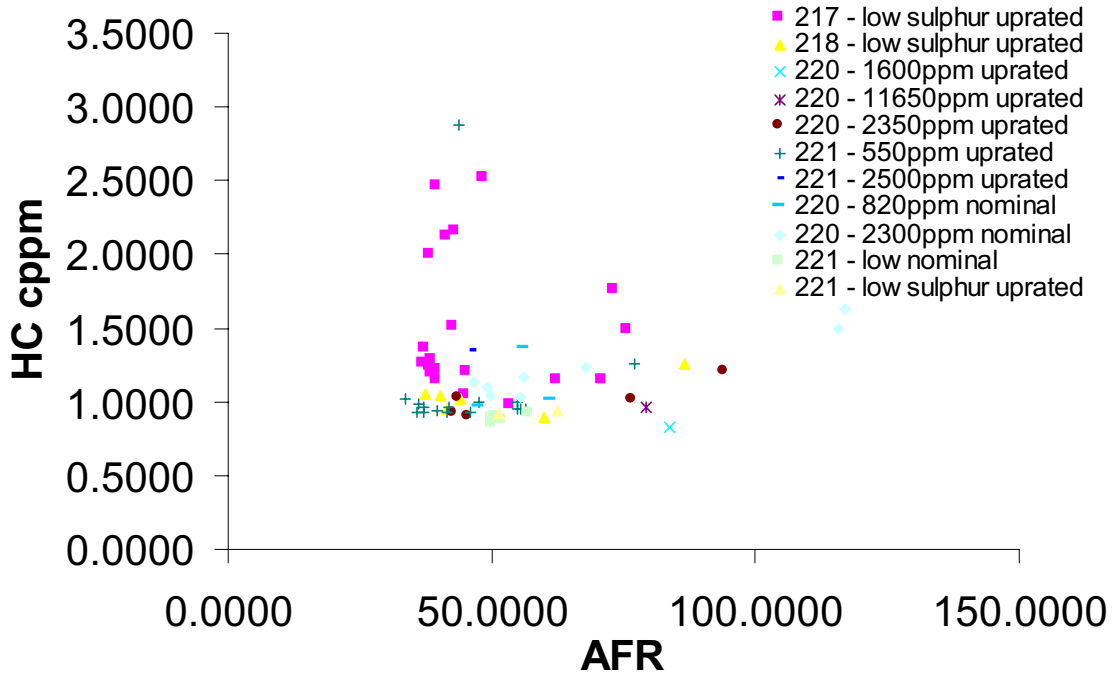

Figure 5 – HC vs AFR for all sulphur levels

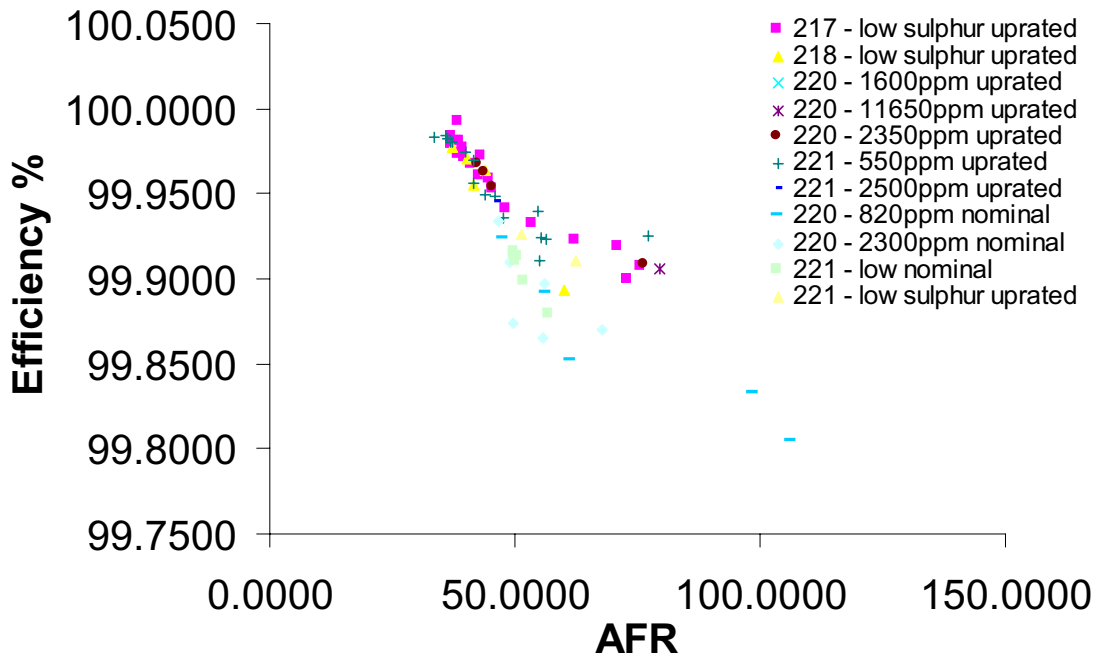

Figure 6 – Efficiency vs AFR for all sulphur levels

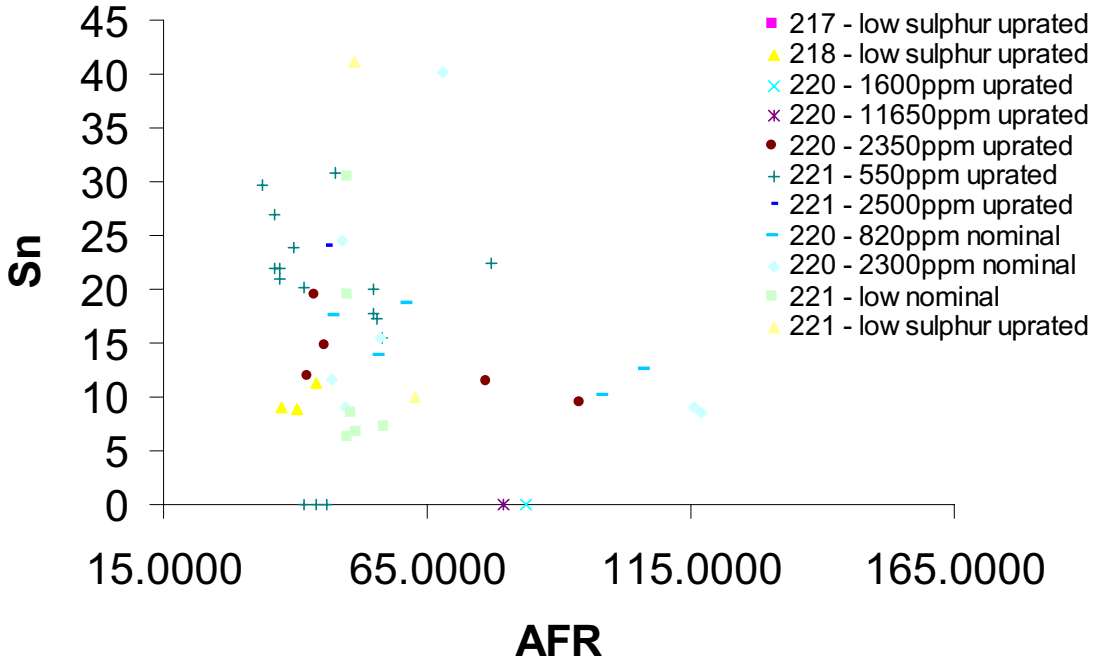

Figure 7 – Sn vs AFR for all sulphur levels

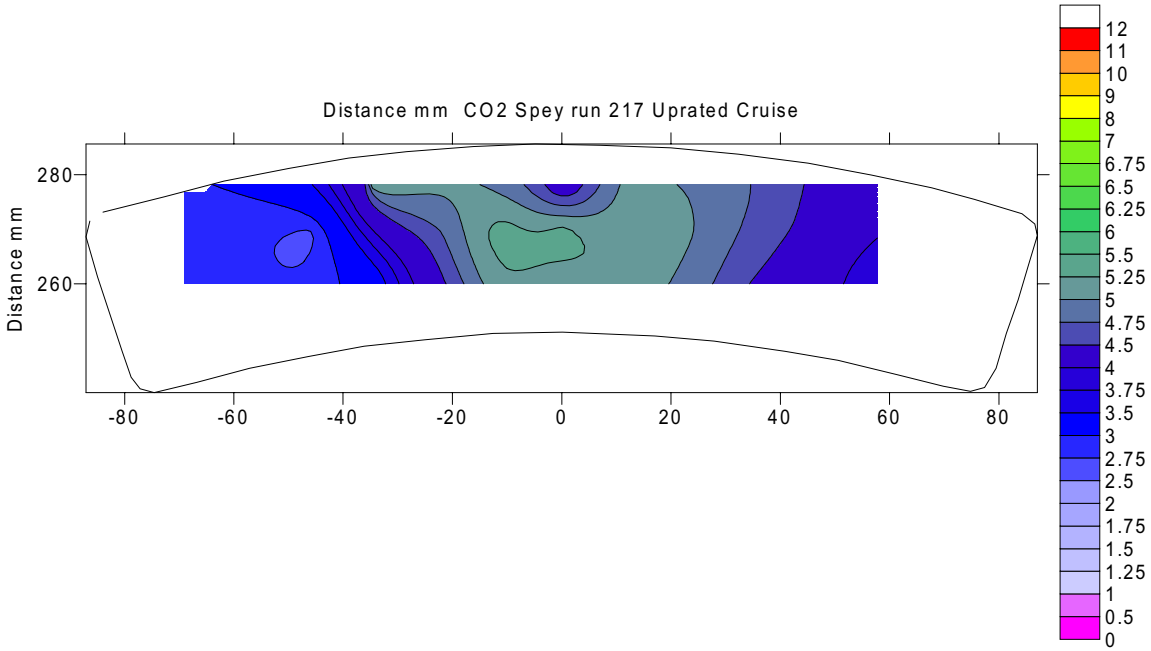

Figure 8 – CO_2 (%) Spatial Data for Specialised Sulphur Probe

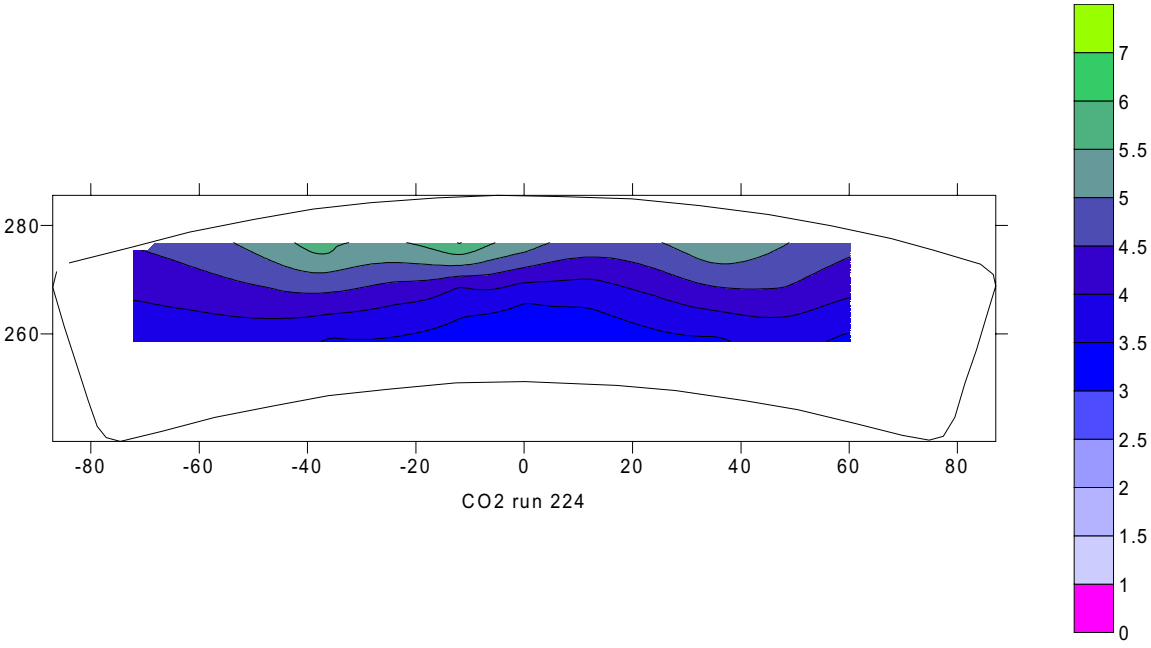

Figure 9 – CO_2 (%) Spatial Data for Standard Probe

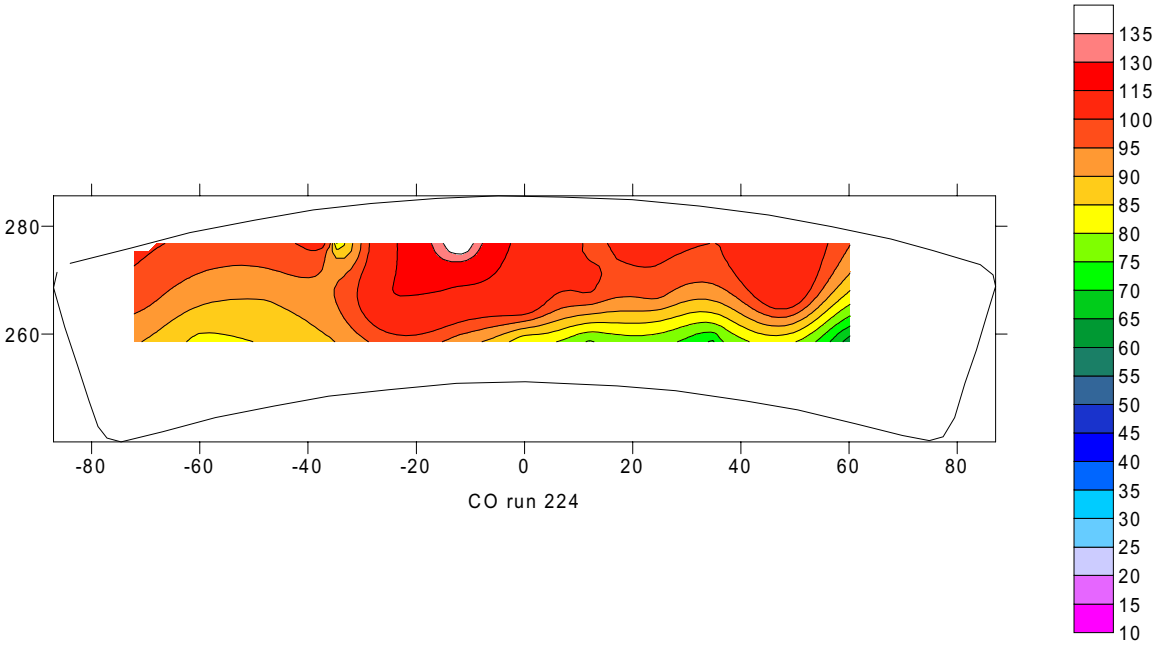

Figure 10 – CO (ppm) Spatial Data for Standard Probe

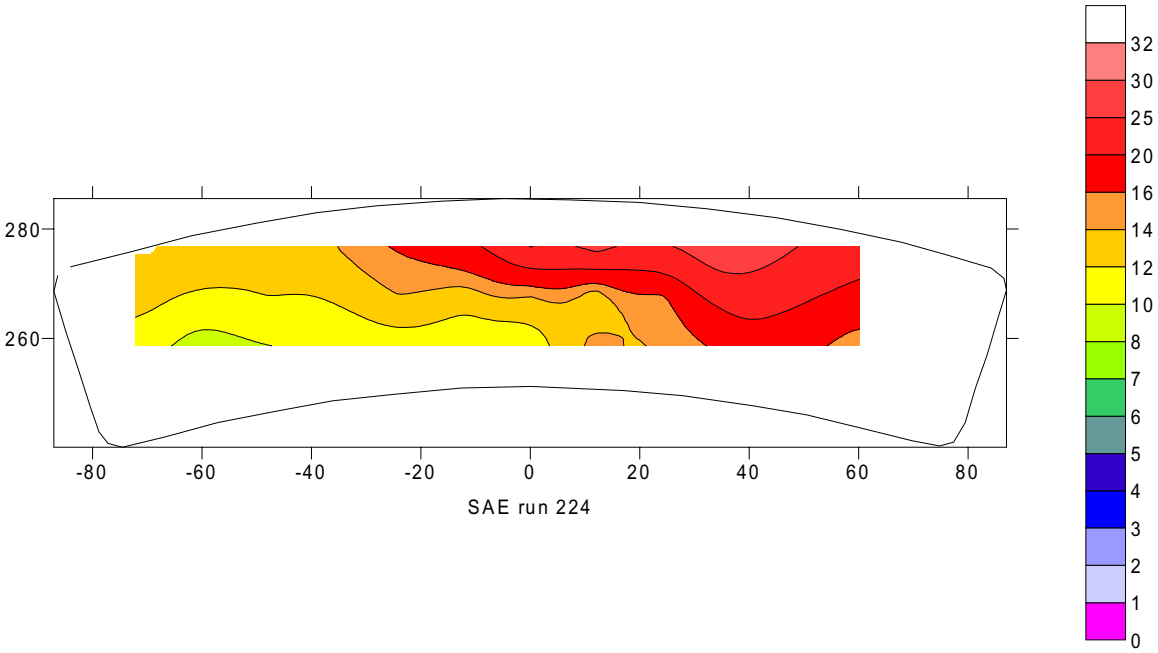

Figure 11 – Smoke Number (SAE) Spatial Data for Standard Probe

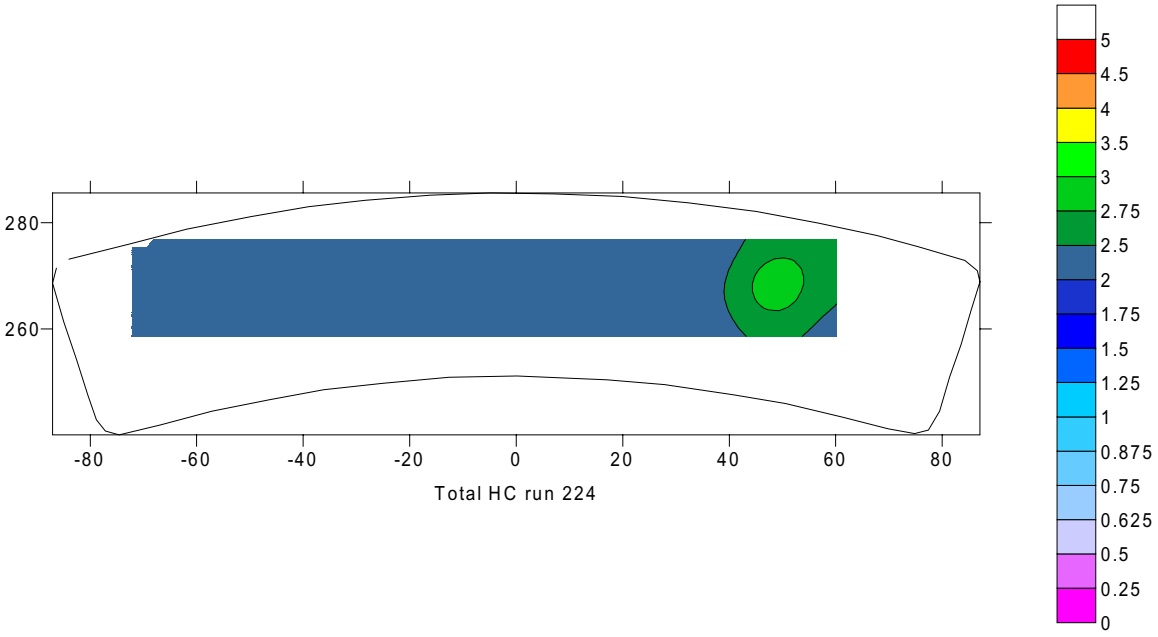

Figure 12 – HC (ppm) Spatial Data for Standard Probe

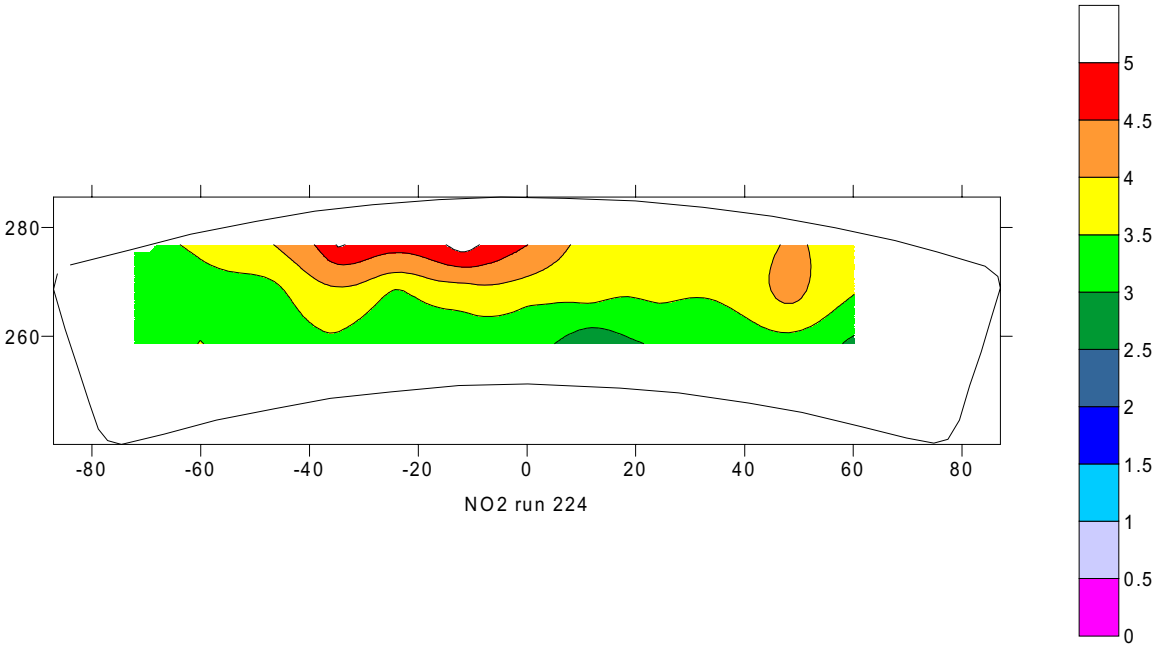

Figure 13 – NO_2 (ppm) Spatial Data for Standard Probe

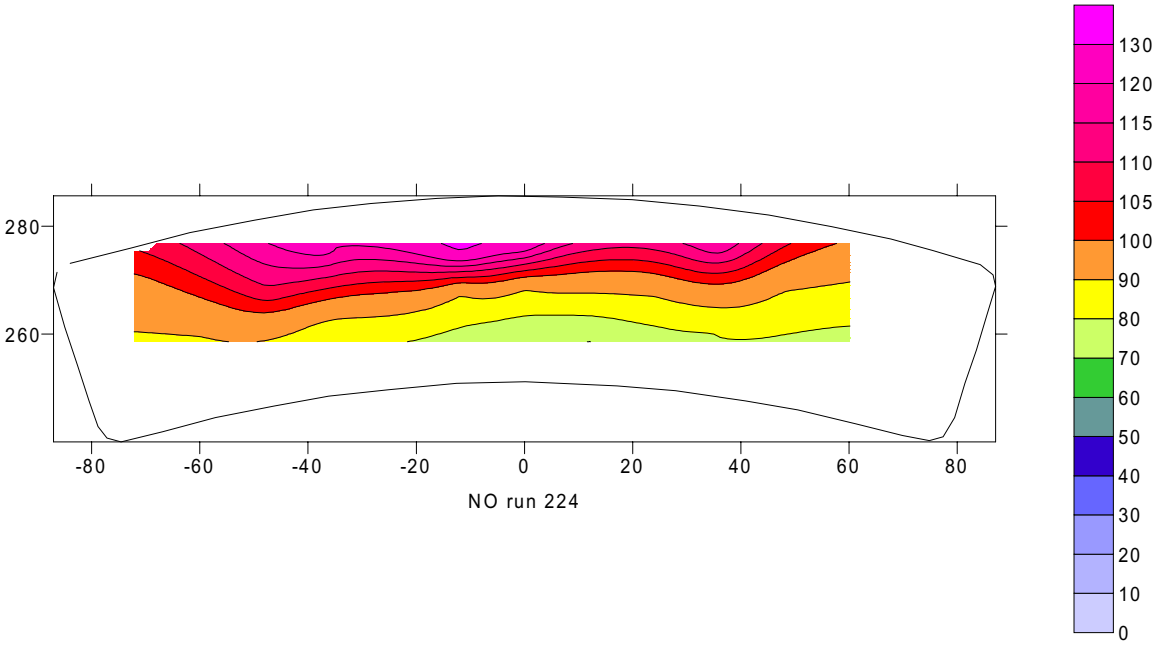

Figure 14 – NO (ppm) Spatial Data for Standard Probe

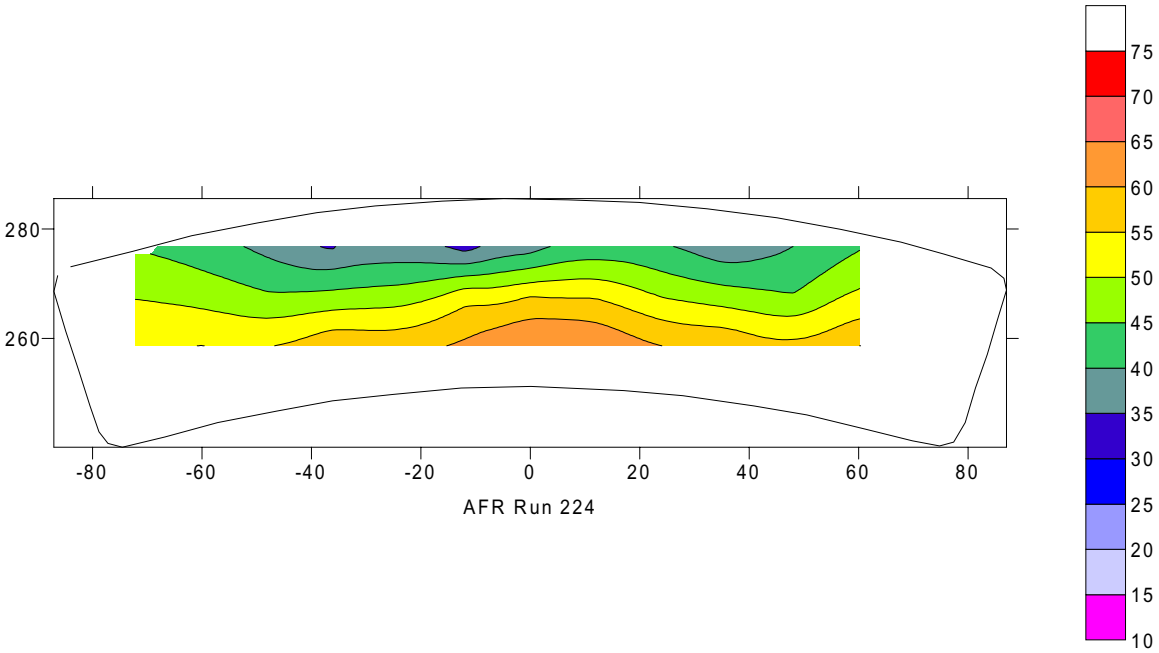

Figure 15 – AFR Spatial Data for Standard Probe

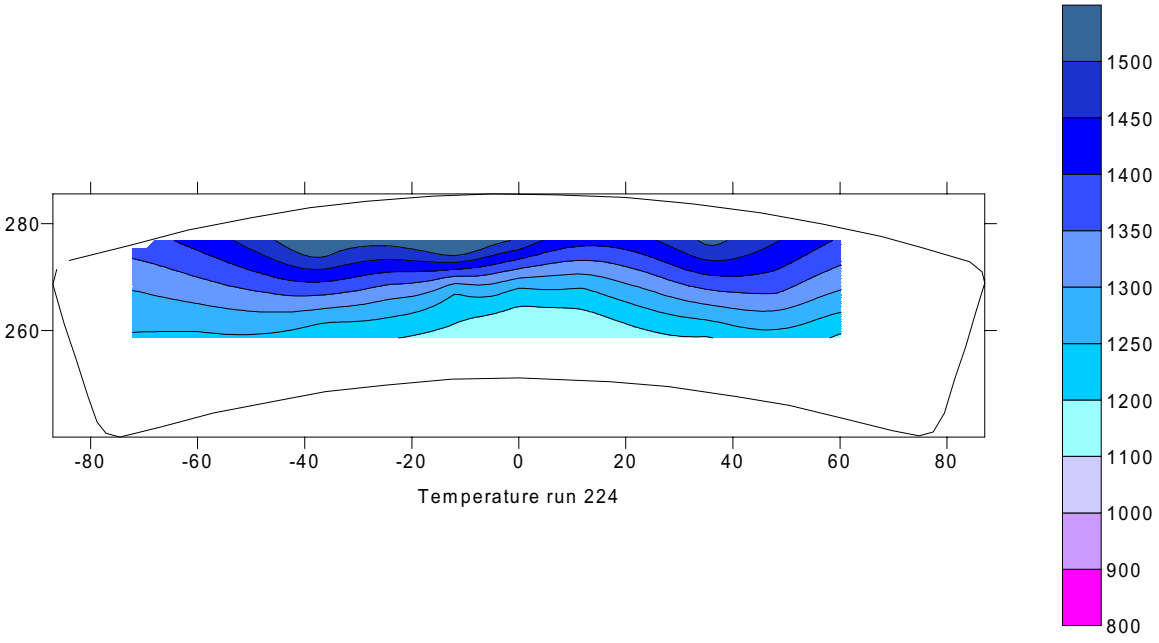

Figure 16 – Temperature (K) Spatial Data for Standard Probe

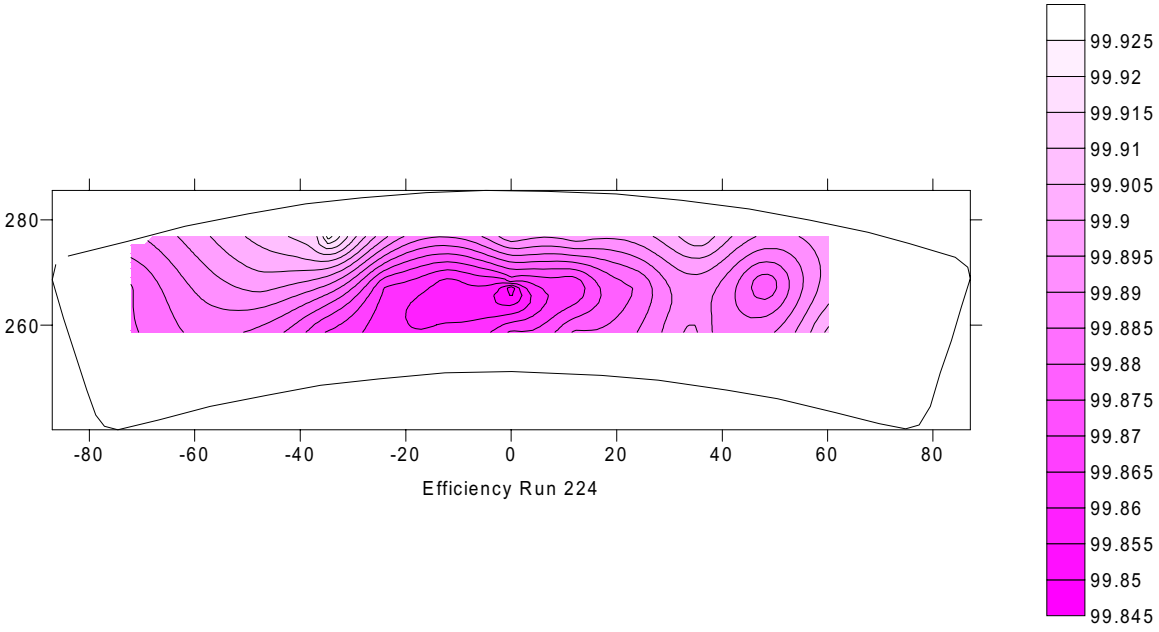

Figure 17 – Efficiency (%) Spatial Data for Standard Probe

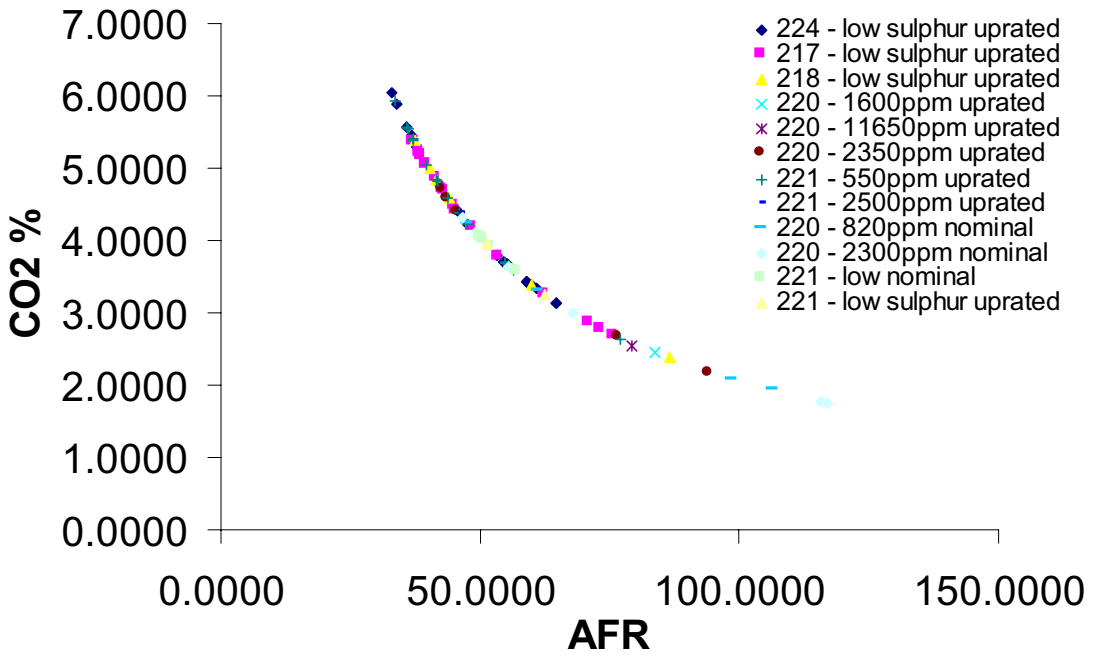

Figure 18 – CO_2 vs AFR for all sulphur levels, both probes

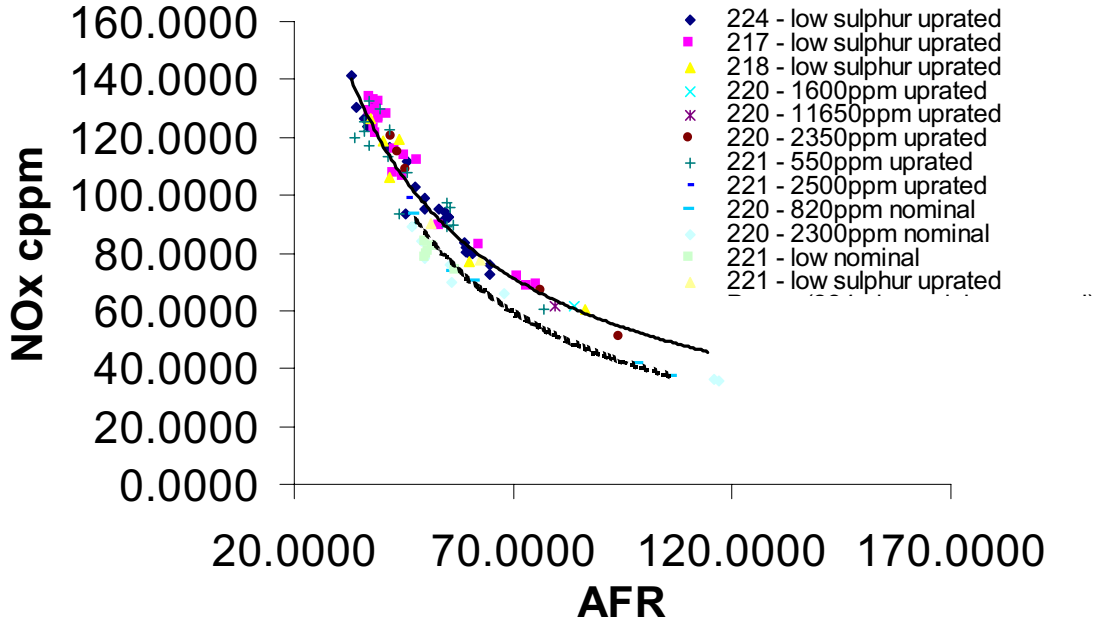

Figure 19 – NO_x vs AFR for all sulphur levels, both probes

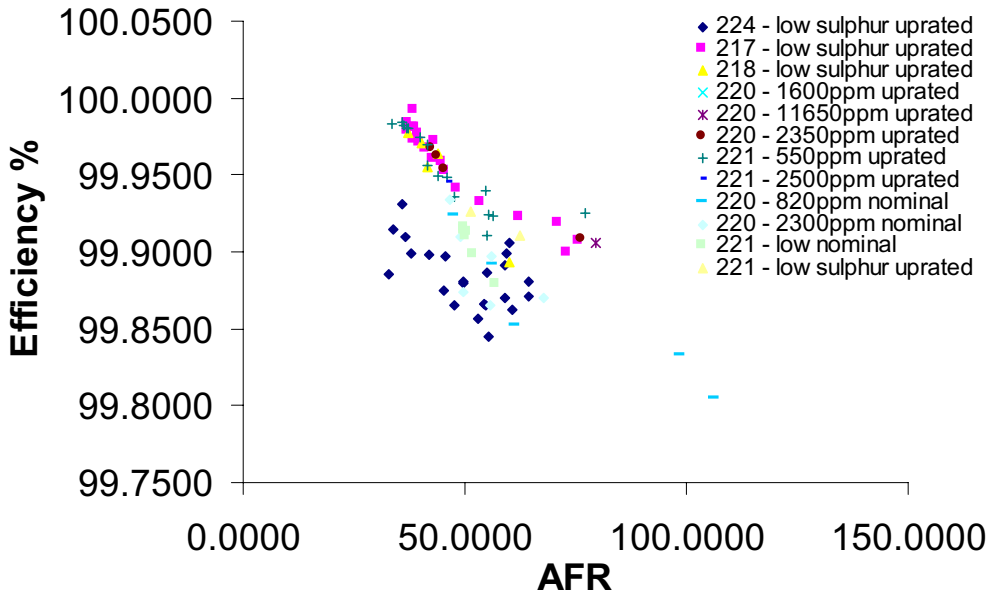

Figure 20 – Efficiency vs AFR for all sulphur levels, both probes

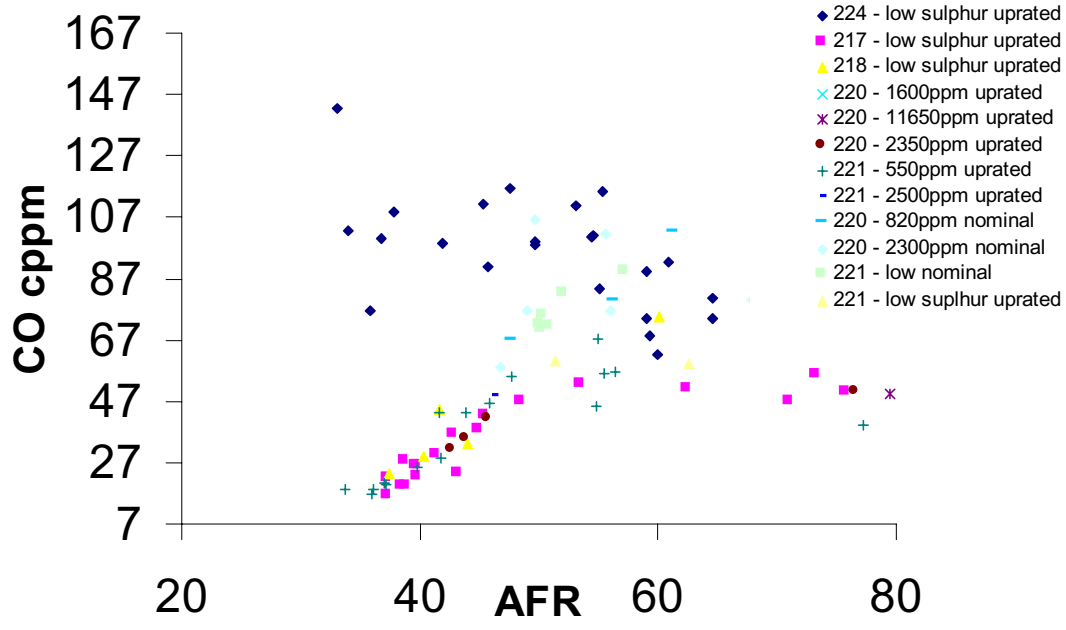

Figure 21 – CO vs AFR for all sulphur levels, both probes

Instrument	LIMS Ref.	Audit due	Range	
Chart Recorder	I7	04/08/01	0–10V	
CO	I21	17/12/00	1%	
CO	I20	17/12/00	15%	
CO	I25	02/08/01	500 & 2500ppm	
CO_2	I40	17/12/00	2%	
CO_2	I35	07/12/00	15%	
NO & NO_x	I143	19/11/00	1000ppm	
HC	I75	17/12/00	1000ppm	
O_2	I87	17/12/00	25%	
Smoke	I118	15/12/00	100 SN	
Reflectometer	I100	25/10/00	10–90%	
Barometer	I145	27/7/01	800–1150mbar	
Dried Sample Hygrometer	I58	15/6/01	–10 to +15 °C	
Inlet Air Hygrometer	I57	8/8/01	–5 to +15 °C	

Table 1 – List of Gas Analysis Instrumentation Utilised During the DERA/NASA Testing

Table 2 – Emissions Data from the DERA/NASA Testing

TIME	Run 217 TEST PT. CODE	16/08/00 SAE	Uprated Cruise CO_2 %	N_2c%	No doping O_2 %	H_2O %	16/08/00 Inlet air Dew Point Deg C	Inlet air humidity expressed as volume of water vapour per volume of dry air	CO ppm	HC ppm C	H_2cp pm	NO_2 ppm	NO ppm	NO_x ppm	Comb eff%	AFR	Temp. K	EICO	EIHC	EINO	$EINO_x$	$EINO_x$ ref	$EINO_x$ 0hum	EINO 0hum
10:09:41	1	No data	5.23	75.22	12.49	6.15	9.66	0.012	5	2	2	1	131	132	100.0	38.5	1488	0.2	0.0	8.3	8.4	8.6	9.7	9.6
10:14:30	2	No data	4.67	75.40	13.36	5.65	10.07	0.012	23	2	12	2	114	116	100.0	43.2	1396	1.0	0.1	8.1	8.2	8.5	9.5	9.4
10:25:23	2 repeated	No data	4.75	75.33	13.23	5.77	10.67	0.013	34	2	17	3	119	123	100.0	42.4	1408	1.4	0.1	8.3	8.6	8.9	10.0	9.7
10:46:22	3	No data	4.17	75.49	14.12	5.29	11.41	0.013	47	3	24	5	107	111	99.9	48.4	1317	2.3	0.1	8.5	8.9	9.3	10.4	10.0
10:59:42	4	No data	5.05	75.15	12.73	6.15	11.69	0.014	26	2	13	4	128	132	100.0	39.8	1456	1.0	0.1	8.4	8.7	9.1	10.2	9.9
11:16:06	5	No data	4.86	75.19	13.03	6.01	12.14	0.014	29	2	15	5	123	128	100.0	41.4	1426	1.2	0.1	8.4	8.7	9.2	10.3	9.9
11:38:38	6	No data	2.78	75.92	16.29	4.08	12.60	0.015	56	2	28	4	64	68	99.9	73.3	1090	4.1	0.1	7.6	8.1	8.6	9.7	9.1
12:09:26	7	No data	2.69	75.89	16.42	4.07	13.39	0.015	50	1	25	5	63	69	99.9	75.7	1075	3.8	0.1	7.8	8.5	9.1	10.2	9.4
12:31:25	8	No data	4.69	75.15	13.26	5.98	13.47	0.015	36	2	18	5	102	107	100.0	42.8	1400	1.6	0.0	7.2	7.6	8.1	9.1	8.7
13:10:13	2 repeated	No data	5.04	74.95	12.70	6.39	14.37	0.016	35	1	18	6	111	117	100.0	39.8	1454	1.4	0.0	7.3	7.7	8.3	9.4	8.9
13:33:18	9	No data	5.36	74.79	12.18	6.76	14.92	0.017	22	1	11	6	123	129	100.0	37.3	1504	0.8	0.0	7.6	8.0	8.7	9.8	9.4
13:50:33	10	No data	5.37	74.75	12.16	6.81	15.35	0.017	16	1	8	5	129	134	100.0	37.3	1505	0.6	0.0	8.0	8.3	9.1	10.2	9.8
14:07:22	11	No data	5.16	74.82	12.49	6.62	15.40	0.017	19	1	10	5	124	129	100.0	38.8	1472	0.8	0.0	8.0	8.3	9.1	10.3	9.9
14:25:46	12	No data	5.04	74.85	12.67	6.53	15.63	0.018	22	1	11	5	121	127	100.0	39.8	1454	0.9	0.0	8.0	8.3	9.2	10.3	9.9
14:37:43	13	No data	4.42	75.07	13.65	5.95	15.66	0.018	42	1	21	7	106	113	100.0	45.5	1357	1.9	0.0	8.0	8.5	9.4	10.6	9.9
14:58:52	14	No data	2.86	75.64	16.11	4.47	15.66	0.018	47	1	23	5	66	72	99.9	71.1	1104	3.3	0.0	7.7	8.3	9.2	10.4	9.6
15:15:20	15	No data	3.24	75.54	15.51	4.79	15.25	0.017	51	1	25	7	76	83	99.9	62.5	1168	3.2	0.0	7.8	8.5	9.3	10.5	9.6
15:29:41	16	No data	5.17	74.87	12.48	6.56	14.74	0.017	27	1	14	6	115	121	100.0	38.7	1476	1.1	0.0	7.4	7.8	8.4	9.5	9.0
15:44:04	17	No data	5.05	74.94	12.67	6.42	14.49	0.016	26	1	13	6	120	126	100.0	39.7	1457	1.0	0.0	7.9	8.3	8.9	10.1	9.6
16:00:12	18	No data	5.21	74.90	12.43	6.54	14.23	0.016	19	1	10	5	118	122	100.0	38.5	1481	0.7	0.0	7.5	7.8	8.4	9.5	9.1
16:11:47	19	No data	4.48	75.19	13.58	5.82	13.93	0.016	38	1	19	6	99	106	100.0	44.9	1368	1.7	0.0	7.4	7.8	8.4	9.5	8.9
16:25:45	20	No data	3.77	75.44	14.70	5.17	14.08	0.016	53	1	26	7	83	89	99.9	53.5	1256	2.8	0.0	7.3	7.9	8.5	9.5	8.8

Table 2 – Continued.

	Run 218		Uprated Cruise		No doping			18/08/00														
TIME	TEST PT. CODE	SAE	CO_2 %	N_2c%	O_2 %	H_2O %	Inlet air Dew Point Deg C	Inlet air humidity expressed as volume of water vapour per volume of dry air	CO ppm	HC ppm C	H_2cp pm	NO_2 ppm	NO ppm	NO_x ppm	Comb eff%	AFR	Temp. K	EICO	EIHC	EINO	$EINO_x$	$EINO_x$ ref	$EINO_x$ 0hum	EINO 0hum
14:48:32	7	No data	2.38	76.35	17.01	3.34	8.41	0.011	49	1	24	3	57	61	99.9	86.5	1022	4.2	0.1	8.1	8.5	8.6	9.7	9.2
15:06:51	8	No data	3.39	75.89	15.39	4.40	9.82	0.012	74	1	37	5	72	77	99.9	60.0	1194	4.4	0.0	7.0	7.6	7.8	8.8	8.2
15:27:48	9	No data	4.84	75.29	13.10	5.85	10.79	0.013	44	1	22	5	101	106	100.0	41.7	1419	1.8	0.0	6.9	7.3	7.5	8.5	8.1
16:01:30	10	9	5.38	75.15	12.26	6.30	10.03	0.012	24	1	12	4	123	127	100.0	37.4	1506	0.9	0.0	7.6	7.8	8.0	9.1	8.8
16:09:17	12	9	5.01	75.29	12.85	5.93	9.86	0.012	29	1	15	4	115	119	100.0	40.3	1450	1.2	0.0	7.6	7.9	8.1	9.1	8.8
16:26:05	13	11	4.60	75.47	13.50	5.52	9.74	0.012	33	1	17	5	114	119	100.0	44.0	1386	1.5	0.0	8.3	8.6	8.8	9.9	9.5

	Run 220		Uprated Cruise		1600 ppm so2			22/08/00														
TIME	TEST PT. CODE	SAE	CO_2 %	N_2c%	O_2 %	H_2O %	Inlet air Dew Point Deg C	Inlet air humidity expressed as volume of water vapour per volume of dry air	CO ppm	HC ppm C	H_2cp pm	NO_2 ppm	NO ppm	NO_x ppm	Comb eff%	AFR	Temp. K	EICO	EIHC	EINO	$EINO_x$	$EINO_x$ ref	$EINO_x$ 0hum	EINO 0hum
10:28:41	1	SAE	2.44	76.25	16.89	3.49	9.62	0.012	44	1	22	4	58	62	99.9	83.8	1031	3.6	0.0	7.9	8.4	8.6	9.7	9.1

	Run 220		Uprated Cruise		11650 ppm so2			22/08/00														
TIME	TEST PT. CODE	SAE	CO_2 %	N_2c%	O_2 %	H_2O %	Inlet air Dew Point Deg C	Inlet air humidity expressed as volume of water vapour per volume of dry air	CO ppm	HC ppm C	H_2cp pm	NO_2 ppm	NO ppm	NO_x ppm	Comb eff%	AFR	Temp. K	EICO	EIHC	EINO	$EINO_x$	$EINO_x$ ref	$EINO_x$ 0hum	EINO 0hum
10:06:22	1	No data	2.55	76.26	16.71	3.54	8.67	0.011	49	1	0	4	58	61	99.9	79.4	1052	3.9	0.0	7.5	7.9	8.0	9.1	8.5

	Run 220		Uprated Cruise		2350 ppm so2			22/08/00														
TIME	TEST PT. CODE	SAE	CO_2 %	N_2c%	O_2 %	H_2O %	Inlet air Dew Point Deg C	Inlet air humidity expressed as volume of water vapour per volume of dry air	CO ppm	HC ppm C	H_2cp pm	NO_2 ppm	NO ppm	NO_x ppm	Comb eff%	AFR	Temp. K	EICO	EIHC	EINO	$EINO_x$	$EINO_x$ ref	$EINO_x$ 0hum	EINO 0hum
15:21:33	7	9	2.16	76.05	17.24	3.62	13.90	0.016	43	1	22	3	47	50	99.9	94.3	987	4.0	0.1	7.3	7.8	8.3	9.4	8.8
15:42:04	8	11	2.65	75.84	16.46	4.13	14.30	0.016	50	1	25	5	62	66	99.9	76.6	1071	3.8	0.0	7.7	8.3	9.0	10.1	9.4
16:01:14	10	15	4.38	75.16	13.71	5.82	14.76	0.017	41	1	21	5	103	108	100.0	45.8	1354	1.9	0.0	7.8	8.2	8.9	10.0	9.5
16:14:03	12	12	4.69	75.04	13.22	6.13	14.88	0.017	31	1	16	5	115	120	100.0	42.7	1403	1.3	0.0	8.1	8.5	9.2	10.4	9.9
16:31:01	13	19	4.56	75.07	13.42	6.02	15.04	0.017	35	1	17	5	110	114	100.0	43.9	1383	1.5	0.0	8.0	8.3	9.0	10.2	9.8

Table 2 – Continued.

	Run 220		Normal Cruise		830 ppm so2			22/08/00													
TIME	TEST PT. CODE	SAE	CO_2 %	N_2c%	O_2 %	H_2O %	Inlet air Dew Point Deg C	Inlet air humidity expressed as volume of water vapour per volume of dry air	CO ppm	HC ppm C	H_2cp pm	NO_2 ppm	NO ppm	NO_x ppm	Comb eff%	AFR	Temp. K	EICO	EIHC	EINO	$EINO_x$	$EINO_x$ ref	$EINO_x$ 0hum	EINO 0hum
13:21:51	13	14	3.60	75.67	15.02	4.79	11.92	0.014	80	1	40	6	67	73	99.9	56.3	1208	4.5	0.0	6.2	6.8	7.1	8.0	7.3
13:48:33	12	17	4.23	75.40	14.02	5.43	12.40	0.014	67	1	33	6	87	93	99.9	47.7	1310	3.2	0.0	6.8	7.3	7.7	8.7	8.1
14:09:11	10	19	3.30	75.73	15.46	4.58	12.63	0.014	102	1	51	6	64	70	99.9	61.3	1161	6.2	0.0	6.4	7.0	7.4	8.3	7.7
14:27:46	8	12	1.92	76.21	17.64	3.31	13.02	0.015	74	3	37	2	34	37	99.8	106.5	924	7.8	0.2	6.0	6.4	6.8	7.6	7.1
14:40:59	7	10	2.07	76.14	17.40	3.46	13.13	0.015	69	2	34	3	39	41	99.8	98.6	951	6.7	0.1	6.2	6.6	7.1	7.9	7.5
	Run 220		Normal cruise		2300 ppm so2			22/08/00													
TIME	TEST PT. CODE	SAE	CO_2 %	N_2c%	O_2 %	H_2O %	Inlet air Dew Point Deg C	Inlet air humidity expressed as volume of water vapour per volume of dry air	CO ppm	HC ppm C	H_2cp pm	NO_2 ppm	NO ppm	NO_x ppm	Comb eff%	AFR	Temp. K	EICO	EIHC	EINO	$EINO_x$	$EINO_x$ ref	$EINO_x$ 0hum	EINO 0hum
10:58:01	1	9	1.78	76.44	17.92	2.94	10.46	0.013	30	2	15	1	35	36	99.9	115.8	899	3.4	0.1	6.6	6.8	7.0	7.9	7.6
11:27:37	2	40	2.99	75.97	15.99	4.12	10.76	0.013	80	1	40	4	62	66	99.9	67.9	1108	5.4	0.0	6.8	7.3	7.6	8.6	8.0
11:40:52	4	25	4.11	75.55	14.21	5.20	10.87	0.013	76	1	38	5	79	84	99.9	49.0	1293	3.7	0.0	6.4	6.8	7.0	7.9	7.4
11:55:50	5	12	4.31	75.47	13.91	5.39	11.02	0.013	58	1	29	5	84	89	99.9	46.8	1324	2.7	0.0	6.5	6.9	7.1	8.0	7.6
12:16:26	7	9	1.76	76.36	17.93	3.03	11.75	0.014	33	2	16	1	34	36	99.9	117.1	894	3.8	0.1	6.5	6.8	7.1	8.0	7.6
12:31:57	10	No data	3.63	75.70	14.97	4.78	11.75	0.014	102	1	51	6	70	76	99.9	55.6	1215	5.6	0.0	6.4	6.9	7.2	8.1	7.5
12:39:35	10	9	4.05	75.53	14.29	5.20	11.46	0.013	106	1	53	7	71	78	99.9	49.7	1284	5.3	0.0	5.8	6.4	6.6	7.5	6.9
12:52:44	13	16	3.61	75.69	15.00	4.77	11.48	0.013	77	1	38	5	65	70	99.9	56.0	1212	4.3	0.0	5.9	6.4	6.7	7.5	7.0
	Run 221		Uprated cruise		550 ppm so2			25/08/00													
TIME	TEST PT. CODE	SAE	CO_2 %	N_2c%	O_2 %	H_2O %	Inlet air Dew Point Deg C	Inlet air humidity expressed as volume of water vapour per volume of dry air	CO ppm	HC ppm C	H_2cp pm	NO_2 ppm	NO ppm	NO_x ppm	Comb eff%	AFR	Temp. K	EICO	EIHC	EINO	$EINO_x$	$EINO_x$ ref	$EINO_x$ 0hum	EINO 0hum
12:00:24	2	31	4.24	75.48	14.03	5.33	11.41	0.013	55	1	0	5	86	90	99.9	47.7	1327	2.6	0.0	6.7	7.1	7.4	8.3	7.9
12:22:29	3	30	5.94	74.85	11.35	6.94	11.51	0.013	18	1	0	3	117	120	100.0	33.7	1591	0.6	0.0	6.5	6.7	7.0	7.9	7.7
13:02:38	10	27	5.56	74.93	11.94	6.66	12.35	0.014	18	1	0	4	122	125	100.0	36.1	1532	0.7	0.0	7.3	7.5	7.9	8.9	8.6
13:13:45	9	21	5.39	74.97	12.19	6.53	12.66	0.015	20	1	0	4	129	132	100.0	37.2	1508	0.7	0.0	7.9	8.1	8.6	9.7	9.4
13:33:37	8	24	5.05	75.09	12.73	6.22	12.76	0.015	25	1	0	4	126	130	100.0	39.8	1455	1.0	0.0	8.3	8.5	9.0	10.2	9.9
13:44:21	22	22	5.41	74.97	12.16	6.54	12.61	0.014	21	1	0	3	114	117	100.0	37.1	1510	0.8	0.0	7.0	7.2	7.6	8.6	8.3
14:05:30	7	22	5.57	74.92	11.91	6.68	12.47	0.014	17	1	0	3	119	122	100.0	36.0	1535	0.6	0.0	7.1	7.3	7.7	8.6	8.4
14:17:23	21	20	4.84	75.19	13.06	5.99	12.46	0.014	43	1	0	5	109	113	100.0	41.6	1423	1.8	0.0	7.4	7.8	8.2	9.2	8.9
14:31:19	6	22	2.65	75.99	16.52	3.92	12.47	0.014	39	1	0	3	58	61	99.9	77.2	1067	3.0	0.1	7.3	7.6	8.0	9.1	8.7
14:47:22	14	17	3.65	75.62	14.94	4.88	12.54	0.014	56	1	0	5	90	96	99.9	55.5	1234	3.1	0.0	8.2	8.7	9.2	10.4	9.8
14:57:57	15	18	3.70	75.62	14.87	4.90	12.30	0.014	45	1	0	5	84	89	99.9	54.8	1241	2.5	0.0	7.6	8.0	8.4	9.5	9.0
15:10:41	16	16	3.59	75.64	15.03	4.82	12.50	0.014	57	1	0	6	84	90	99.9	56.4	1225	3.2	0.0	7.8	8.3	8.7	9.9	9.2
15:24:08	17	20	3.68	75.59	14.88	4.93	12.73	0.015	67	1	0	7	91	98	99.9	55.0	1239	3.7	0.0	8.2	8.8	9.3	10.5	9.8
12:27:32	repeat 3	No data	4.59	75.34	13.47	5.68	11.60	0.014	43	3	0	4	90	93	99.9	43.9	1384	1.9	0.1	6.5	6.7	7.0	7.9	7.6
15:31:16	repeat 10	No data	4.82	75.17	13.09	6.00	12.78	0.015	28	1	0	5	118	123	100.0	41.8	1419	1.2	0.0	8.1	8.5	9.0	10.1	9.7
15:43:03	repeat 22	No data	4.39	75.30	13.76	5.63	13.07	0.015	46	1	0	5	102	108	99.9	45.9	1352	2.1	0.0	7.7	8.1	8.6	9.7	9.3

Table 2 – Concluded.

			Uprated cruise		2500 ppm so2			25/08/00															
TIME	TEST PT. CODE	SAE	CO_2 %	N_2c%	O_2 %	H_2O %	Inlet air Dew Point Deg C	Inlet air humidity expressed as volume of water vapour per volume of dry air	CO ppm	HC ppm C	H_2cp pm	NO_2 ppm	NO ppm	NO_x ppm	Comb eff%	AFR	Temp. K	EICO	EIHC	EINO	$EINO_x$	$EINO_x$ ref	$EINO_x$ 0hum	EINO 0hum
11:24:19	10	24	4.35	75.48	13.85	5.39	10.73	0.013	48	1	24	5	94	99	99.9	46.3	1347	2.2	0.0	7.1	7.5	7.8	8.8	8.3
	Run 221		Nominal cruise		No doping			25/08/00															
TIME	TEST PT. CODE	SAE	CO_2 %	N_2c%	O_2 %	H_2O %	Inlet air Dew Point Deg C	Inlet air humidity expressed as volume of water vapour per volume of dry air	CO ppm	HC ppm C	H_2cp pm	NO_2 ppm	NO ppm	NO_x ppm	Comb eff%	AFR	Temp. K	EICO	EIHC	EINO	$EINO_x$	$EINO_x$ ref	$EINO_x$ 0hum	EINO 0hum
10:13:10	6	7	3.56	75.91	15.15	4.46	8.55	0.011	90	1	45	4	70	74	99.9	57.1	1197	5.1	0.0	6.5	6.9	7.0	7.9	7.4
10:17:44	21	7	3.90	75.77	14.60	4.80	8.85	0.011	82	1	41	5	77	82	99.9	52.0	1253	4.3	0.0	6.6	7.0	7.1	8.0	7.5
10:21:54	7	6	4.04	75.70	14.38	4.95	9.04	0.011	70	1	35	4	79	84	99.9	50.1	1276	3.5	0.0	6.5	6.9	7.0	7.9	7.5
10:28:04	8	8	3.99	75.71	14.46	4.92	9.29	0.012	72	1	36	5	76	80	99.9	50.8	1271	3.6	0.0	6.3	6.7	6.8	7.7	7.3
10:32:32	9	30	4.02	75.68	14.40	4.97	9.50	0.012	75	1	37	5	74	79	99.9	50.4	1277	3.8	0.0	6.1	6.5	6.7	7.5	7.1
10:36:55	10	19	4.05	75.66	14.36	5.01	9.70	0.012	72	1	36	5	73	78	99.9	50.1	1280	3.6	0.0	6.0	6.4	6.6	7.4	6.9
	Run 221		Uprated cruise		No doping			25/08/00															
TIME	TEST PT. CODE	SAE	CO_2 %	N_2c%	O_2 %	H_2O %	Inlet air Dew Point Deg C	Inlet air humidity expressed as volume of water vapour per volume of dry air	CO ppm	HC ppm C	H_2cp pm	NO_2 ppm	NO ppm	NO_x ppm	Comb eff%	AFR	Temp. K	EICO	EIHC	EINO	$EINO_x$	$EINO_x$ ref	$EINO_x$ 0hum	EINO 0hum
11:04:58	10	41	3.95	75.66	14.51	4.96	10.34	0.012	60	1	0	6	84	90	99.9	51.3	1280	3.1	0.0	7.0	7.6	7.8	8.8	8.2
11:11:45	6	10	3.26	75.90	15.60	4.32	10.47	0.013	59	1	0	6	72	78	99.9	62.5	1167	3.7	0.0	7.4	7.9	8.2	9.2	8.6

Table 3 – Density Averaged Emissions Data from the Sulphur and Standard Probe

Run 217	Sulphur Probe																		
	CO_2c%	N_2c%	O_2c%	H2Oc%	COcppm	HCcppmC	H_2cppm	NO_2cppm	NOcppm	NO_xcppm	Combeff%	AFR	Temp.K	EICO	EIHC	EINO	$EINO_x$	$EINO_x$ ref	$EINO_x$ 0hum	EINO 0hum
Mesured	4.36	75.25	13.78	5.69	34.16	2	0	5	103	108	99.96	46.15	1346	1.6	0.0	7.8	8.2	8.8	10.0	9.5
Equilibrium	4.40												1355							

Run 224	Standard Probe																		
	CO_2c%	N_2c%	O_2c%	H2Oc%	COcppm	HCcppmC	H_2cppm	NO_2cppm	NOcppm	NO_xcppm	Combeff%	AFR	Temp.K	EICO	EIHC	EINO	$EINO_x$	$EINO_x$ ref	$EINO_x$ 0hum	EINO 0hum
Mesured	4.09	75.40	14.22	5.36	94.49	2	0	4	94	98	99.89	49.29	1303	4.7	0.1	7.6	7.9	8.4	9.5	9.1
Equilibrium	4.16												1311							

B Appendix—UMR Emissions Measurements

Philip D. Whitefield and Donald E. Hagen
Cloud and Aerosol Sciences Laboratory
University of Missouri-Rolla
Norwood Hall G-7
Rolla, MO 65401

1 March 2001

B.1 Introduction

NASA – DERA Combustor Particulate Emissions Measurements August 2000

As a component of the "NASA – DERA Combustor Emissions Testing in August 2000" project, the Cloud and Aerosol Sciences Laboratory University of Missouri-Rolla performed the following measurements on the particulate emissions as a function of the test matrix (described above):

- total particulate number density (TCN) at the source (i.e. in the combustor)
- number-based particulate size distributions for diameters ranging from 10nm to 1000nm (1μm).

A description of the experimental methodology underlying these measurements has been given in the literature (Whitefield, P.D., M.B. Trueblood, and D.E. Hagen, "Size and hydration characteristics of laboratory simulated jet engine combustion aerosols," Particulate Sci. and Tech. 11, 25 (1993); Hagen, D.E. and P.D. Whitefield, "Particulate emissions in the exhaust plume from commercial jet aircraft under cruise conditions," J. Geophys. Res, Atmos. 101, 19551 (1996)). Analysis of these measurements has provided a set of derived particulate emission parameters that include number- and mass-based emission indices and concentrations, and shape related parameters extracted from the size distributions. These derived data and a discussion of their correlation with other test parameters are presented in section B 4.0.

B.2 Experimental Set Up

A schematic diagram of the UMR diagnostic facility employed in these measurements is given in figure (1). The source emission was extractively sampled from the exit plane of the combustor at elevated pressure (7–8 bar). It was immediately diluted with particle free dry air at 150 °C with typical dilution ratios ranging from 7:1 to 10:1 (red section of schematic). This dilutions serves two purposes: first to inhibit any condensation in the sampling line and secondly to reduce the concentration of particulate arriving at the diagnostic facility. Once diluted, but still at elevated pressure the total particulate concentration and size distribution for particle diameters >800nm was measured in real-time with a High Pressure Large Particle Counter (HPLPC) (blue section of schematic). After passing through the HPLPC the sample underwent a controlled depressurization to 1 bar for further analysis (yellow section of schematic). Total particulate number density in the 1 bar sample was measured using commercially available condensation nucleus counters (CNC) (green section of schematic). These measurements were made in real time continuously throughout the test programme. Size distribution data in the diameter range 10–800nm was acquired using differential mobility analysis. The time required to acquire a

typical size distribution was approximately 5 minutes. Experience indicates that shifts in the emission size distribution can occur within a 5 minute time frame. As a result, the differential mobility analysis is performed batch-wise, in quasi-realtime on tank samples acquired typically in less than 30 seconds (orange section of schematic).

B.3 Results and Discussion

Table B–1 is a list of the particulate emissions parameters derived from the measurements described above. The column headings for *Table B–1* are defined as follows:

- Source Conc: The number concentration of particulates at the combustor sample point referenced to 1 atm. pressure (number of particulates per cm^3 of air).
- Xbar: The mean diameter of the size distribution (nm)
- Width: The absolute difference between Xbara and Xbarv (nm). (The larger the value of the width parameter the greater the contribution to the distribution from particles with diameters greater than Xbar).
- Xbara: The mean diameter of the size distribution with respect to particulate surface area (nm).
- Xbarv: The mean diameter of the size distribution with respect to particulate volume (nm).
- Amass: The mass concentration of particulates at the combustor sample point referenced to 1 atm. pressure (micrograms per m^3 of air, particulate assumed to be carbonaceous in composition with spherical morphology and a uniform density of 1.5 g cm^{-3} (amorphous carbon)).
- EIn: Number-based particulate emission index (number of particulates per kilogram of fuel burned).
- EIm: Mass-based particulate emission index (grams of particulate per kilogram of fuel burned where particulate assumed to be carbonaceous in composition, with spherical morphology and a uniform density of 1.5 g cm^{-3} (amorphous carbon)).
- Aarea: Particulate surface area per unit volume of air

Files listing differential number concentrations versus particle diameter for the mean size distributions measured for each test point can be found in the project data archive. A set of four typical size distribution plots, presented as examples of distributions for two separate test points (S220C1T3 loc.13, and S221C1T3 loc. 7) can be found in *Figure B–2* to *Figure B–5*. The data for each test point is presented in dN/dX (linear scale) and dN/d log X (logarithmic scale) format. Correlations between the particulate parameters in *Table B–1* and other test parameters have been investigated and the results are discussed.

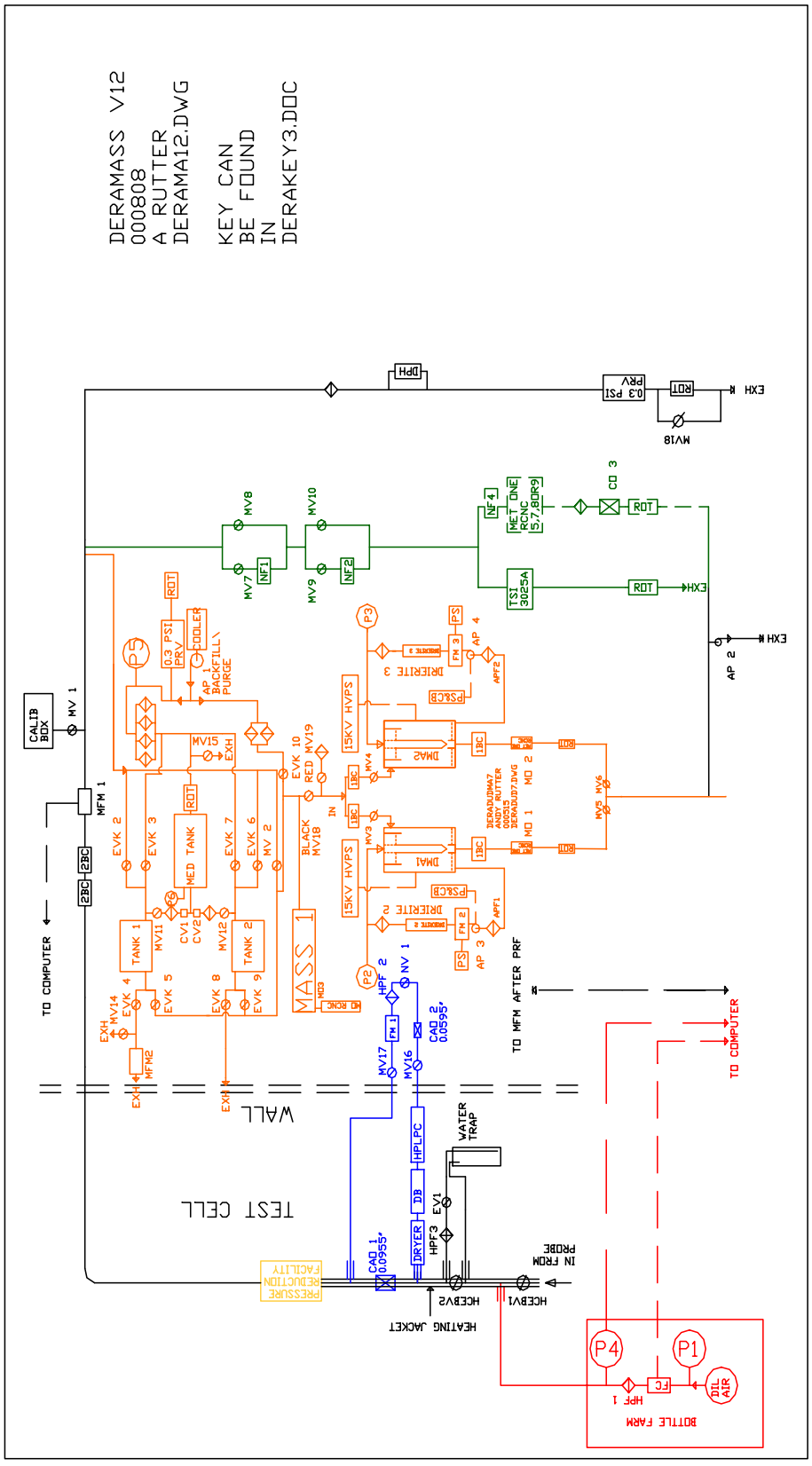

Figure B–1 A schematic diagram of the UMR diagnostic facility

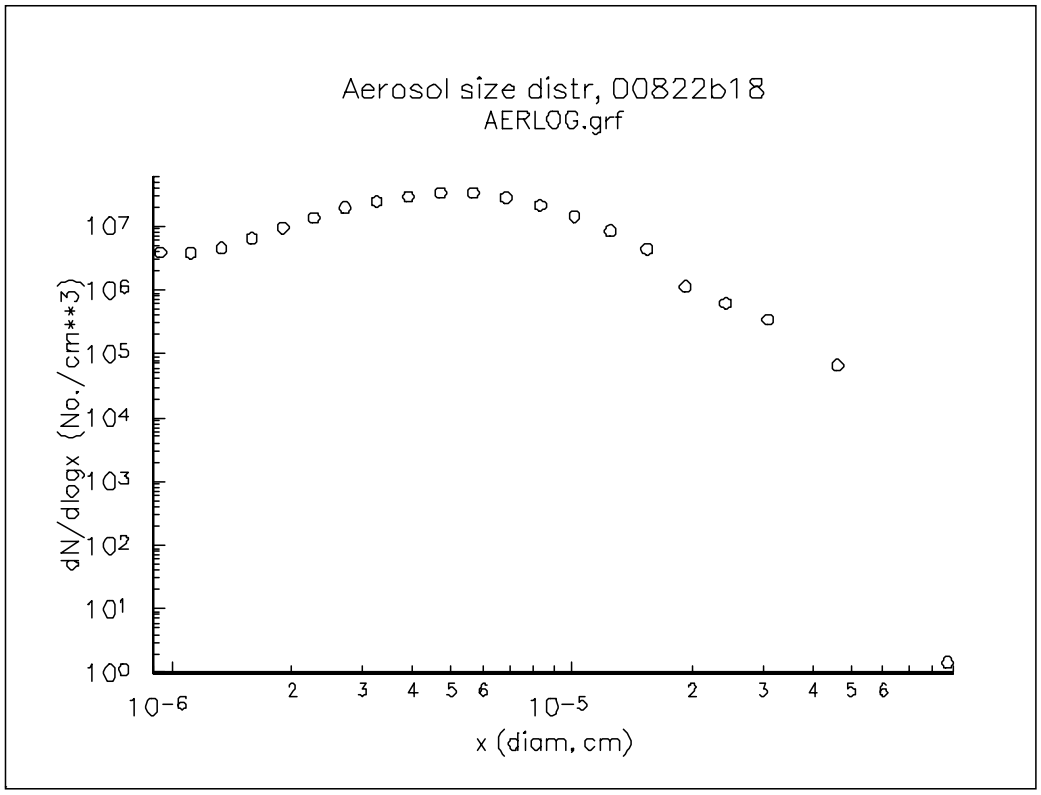

Figure B–2 Example Size Distributions

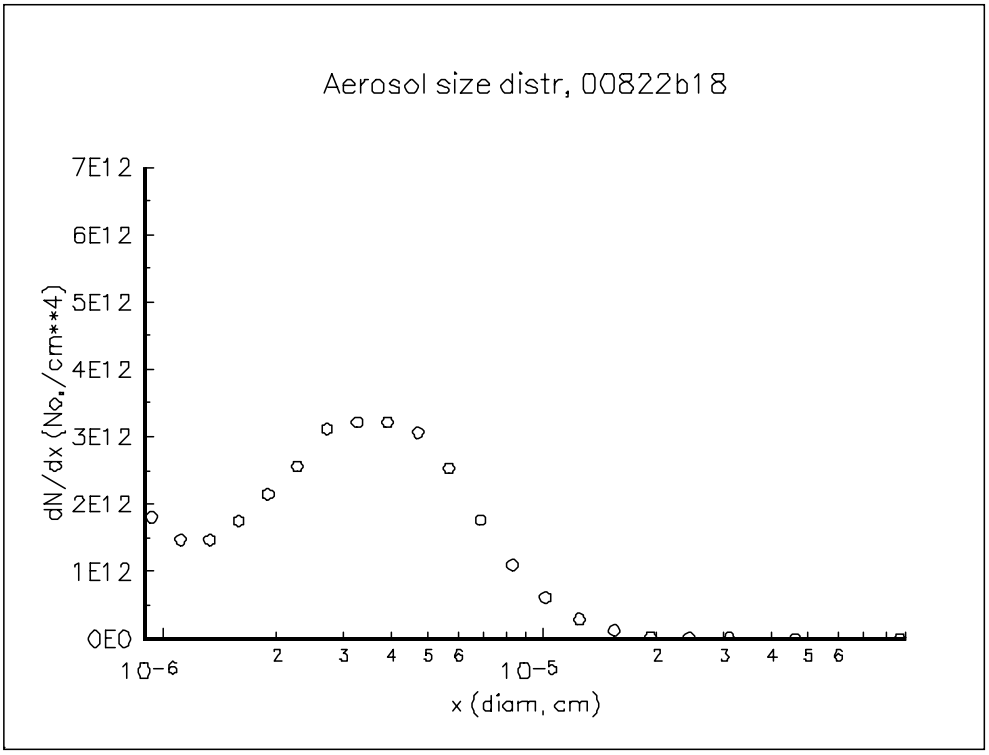

Figure B–3 Example Size Distributions

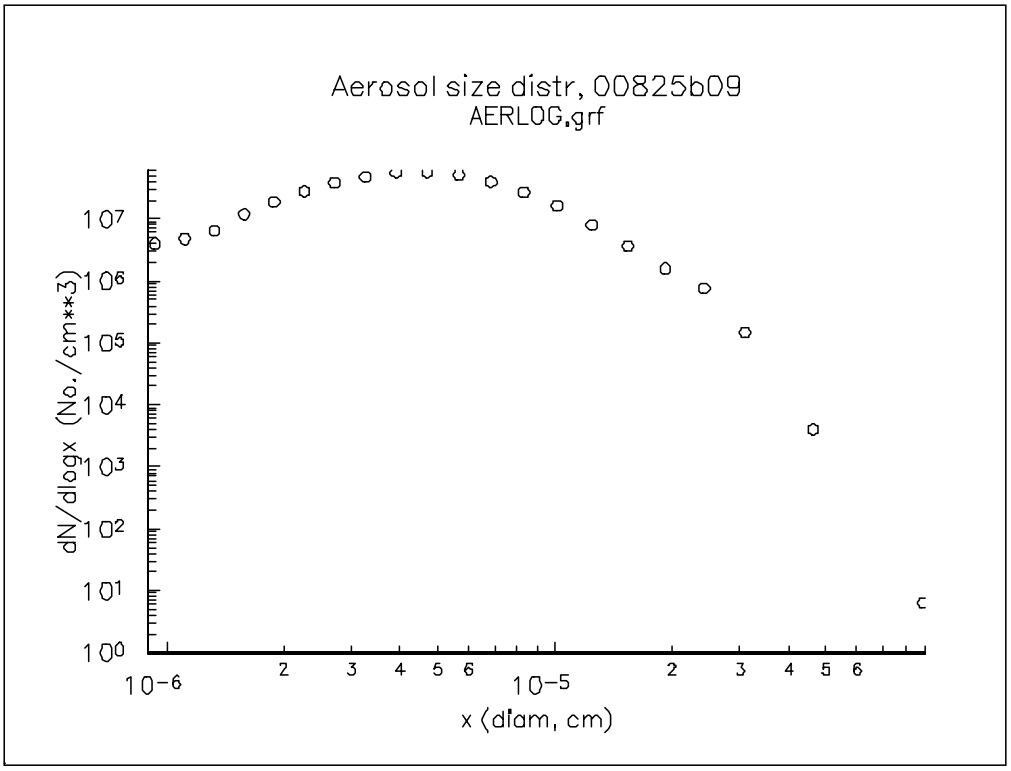

Figure B–4 Example Size Distributions

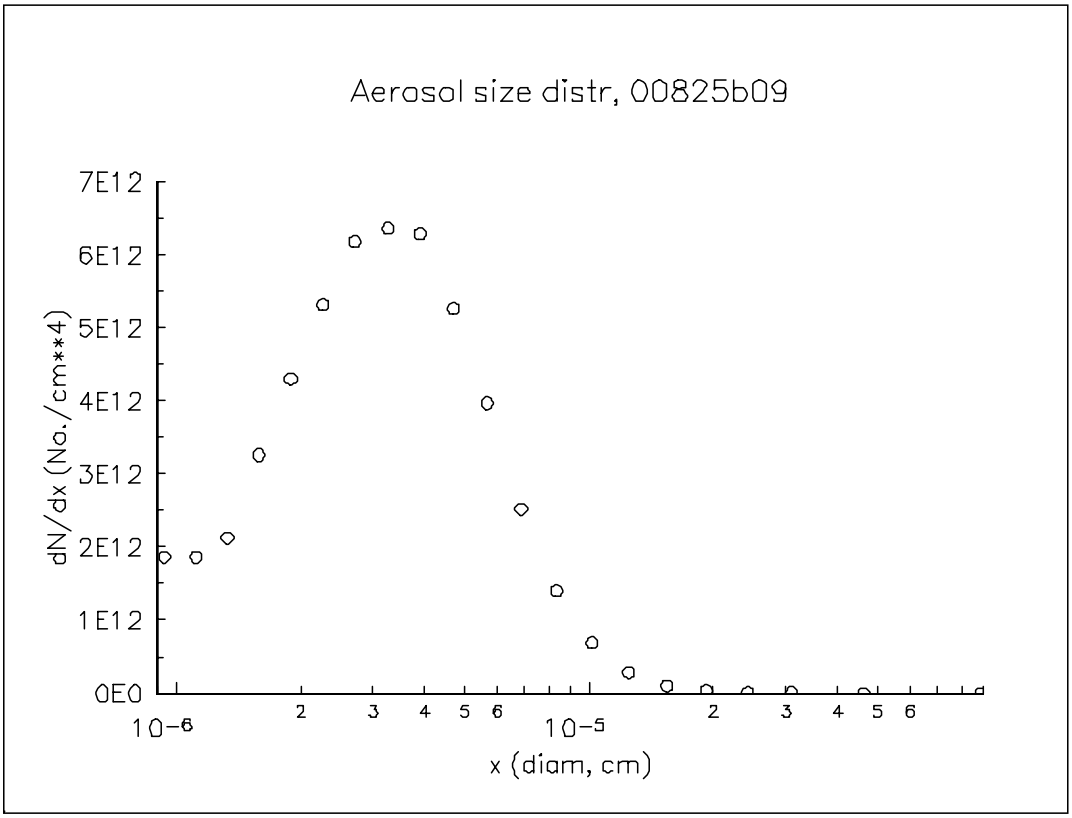

Figure B–5 Example Size Distributions

B.3.1 The impact of varying the fuel sulfur content and power setting

Table B–2 exhibits the effect of variations in fuel sulfur content and power setting upon the exhaust particulate parameters for the combustor. Due to the large variations in the aerosol parameters as a function of probe position the average values for each parameter presented in *Table B–2* have large standard deviation. As a result no statistically significant trends with fuel sulfur content and power setting can be extracted from the averaged data set. Trends may be evident if the aerosol parameters are compared for specific probe positions. Such an analysis is not presented in this report.

B.3.2 Correlation Analysis

The modern gas turbine engine is a complex machine whose performance depends on a large number of parameters, some subject to selection and control by engine design or operator control, e.g. fuel injector size and position, fuel/air ratio, and combustor pressure, and some not

subject to control, e.g., temperature and humidity of the air being ingested for combustion. The dependence of performance on these parameters is not quantitatively understood on a fundamental level, so this dependence is measured experimentally in parameterization studies and the resulting interrelationships are used in engine design, e.g., to enhance engine efficiency and thrust, and in the development of potential mechanisms describing the fate of emittants as they pass from combustor to engine exhaust. The gas phase and particulate emissions naturally depend on these same parameters. The interrelationships between particulate emissions and other gas phase emissions species, as well as with engine operating parameters is of interest. For instance if the fuel flow rate and fuel air ratio is varied to maximize engine efficiency, what does this do to particulate emissions. Or if something is changed in the engine or operations to reduce NOx emissions, what is the concomitant cost in particulate emissions. This type of information can be generated with a multidimensional parameter variation study along with a correlation analysis of the results.

Such an analysis has been performed on a similar data set acquired at the exhaust nozzle exit for a Pratt and Whitney F100 engine (A parametric study of particulate emissions from a modern gas turbine engine, P.D. Whitefield, D.E. Hagen, J. Paladino, Proceedings of the AC23 Workshop, Frankfurt, Germany, July 2000). The DERA data base offers such an opportunity for the study of particulate emissions correlations at the combustor exit plane. These data represent the first measurements to be reported that have been acquired as a function of position in the combustor exit plane. Previous combustor exit plane particulate measurements sponsored by NASA on advanced combustor concepts for the HSCT were made using a fixed position probe.

The particulate parameter dependencies on fuel sulfur content and engine power setting have been explored. The study of other correlations between particulate parameters with gas phase species and engine operating conditions as probe position changed, did not yield any interesting correlations, except for those relating to smoke number (see below). This would indicate that the range of physical and chemical mechanisms associated with the generation of the particulate parameters sampled at different points in the combustor exit plane are not systematically different to a degree that would allow such correlations to be observed.

SAE Smoke Number Correlations. Smoke number correlations with AMass, EIn, EIm, and AArea were tested (see Table B–3). Moderate correlations were observed between smoke number and AMass, EIn, and EIm; and the best correlation was between smoke number and AArea. The scatter plot shown in *Figure B–6* illustrates a case of relatively poor correlation between smoke number and EIm for one operating condition. Many outliers appear at large mass emissions. Theory would suggest the best correlation would be between smoke number and AArea. i.e., the particulate surface area should determine the light reflectance characteristics of the filter paper exposed to the aerosol during the smoke number measurement. This is observed, see Table B–3, last column.

B.3.3 Conclusions from the combustor measurements

A full set of aerosol parameters were obtained as a function of probe position, fuel sulfur content and power. Trends in the probe-position-averaged aerosol parameters were either small or not statistically significant. Moderate correlations between smoke number and aerosol parameters Amass, EIn, EIm, and AArea are reported. No other interesting correlations were observed.

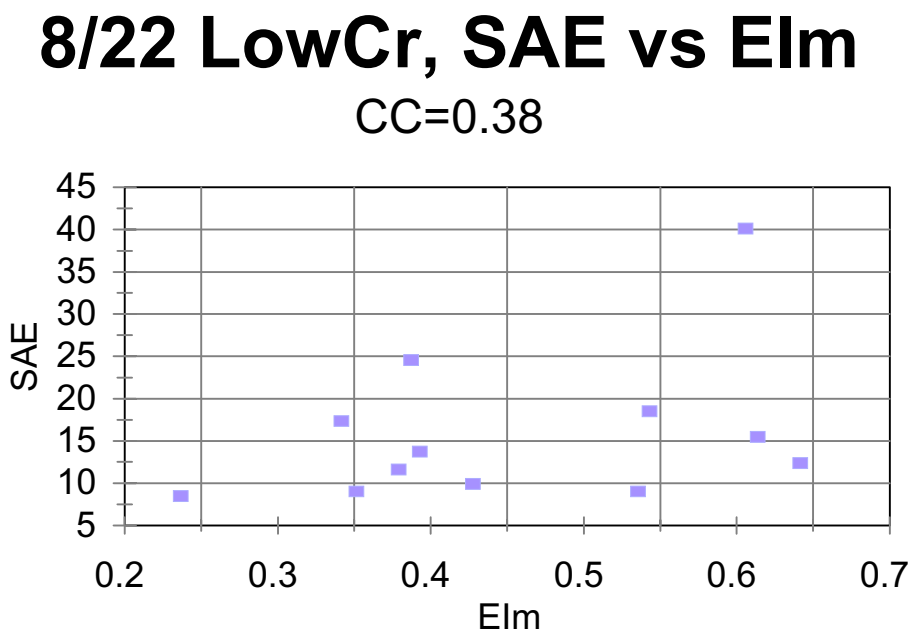
8/22 LowCr, SAE vs Elm
CC=0.38
SAE
45
40
35
30
25
20
15
10
5
0.2
0.3
0.4
0.5
0.6
0.7
Elm

Figure B–6

yymddB	umr ID	Conc (No./cm^3)	Xbar (nm)	Width (nm)	Xbara (nm)	Xbarv (nm)	S_Pt	Sp	Test ID	AMass ug/m3	EIn (No./kg)	EIm (g/kg)	AArea (um2/cm3)
00816b	1	3.057E+06	24.260	34.600	43.720	58.860	1		S217C1T1	623.4664	1.400E+16	2.238E+00	4589.9
	2	2.175E+06	24.380	35.990	44.380	60.360	2			478.3732	8.340E+15	1.440E+00	3365.0
	3	1.667E+06	29.600	39.210	51.670	68.810	3			543.0154	5.380E+15	1.378E+00	3494.8
	4	7.291E+05	29.460	38.890	51.340	68.350	4			232.8137	3.150E+15	7.905E-01	1509.4
	5	3.670E+05	32.700	39.880	55.470	72.570	5			140.2726	1.490E+15	4.486E-01	887.0
	6	1.873E+05	27.650	36.760	48.330	64.410	6			50.04926	3.340E+14	7.006E-02	343.6
	7	5.069E+04	28.860	37.290	49.780	66.150	7			14.67334	8.620E+13	1.959E-02	98.7
	8	6.574E+04	34.300	43.210	58.610	77.510	8			30.61326	2.540E+14	9.289E-02	177.4
	9	2.592E+04	32.860	40.320	55.690	73.180	8	a		10.15927	1.120E+14	3.435E-02	63.1
	10	7.244E+04	32.050	39.760	54.580	71.810	2	a		26.82497	2.850E+14	8.278E-02	169.5
	11	2.033E+04	29.050	37.110	49.970	66.150	9			5.884446	9.640E+13	2.191E-02	39.9
	12	1.832E+03	29.110	37.090	50.040	66.190	10			0.531196	8.690E+12	1.980E-03	3.6
	13	4.627E+03	28.220	37.450	49.540	65.670	11			1.310248	2.060E+13	4.589E-03	8.9
	14	2.151E+04	30.050	40.520	52.950	70.570	12			7.56104	9.260E+13	2.556E-02	47.4
	15	1.105E+05	30.740	39.190	52.960	69.930	13			37.79133	3.890E+14	1.046E-01	243.4
	16	6.536E+05	28.640	36.620	49.430	65.270	14			181.7354	1.210E+15	2.646E-01	1254.2
	17	1.776E+06	27.040	36.460	47.470	63.500	15			454.8178	3.950E+15	7.942E-01	3143.7
	18	2.497E+05	34.620	47.590	60.620	82.210	16			138.7148	1.120E+15	4.888E-01	720.6
	19	5.461E+05	28.970	36.130	49.570	65.100	17			150.6742	2.360E+15	5.121E-01	1054.0
	20	3.073E+05	31.500	39.430	53.750	70.930	18			109.6432	1.390E+15	3.904E-01	697.2
	21	2.100E+05	31.940	38.530	54.260	70.470	19			73.50115	7.57E+14	0.207993	485.7
	22	1.104E+05	29.510	34.460	49.390	63.970	20			28.89478	3.070E+14	6.319E-02	211.5

yymddB	umr ID	Source Conc (No./cm^3)	UMR_Res Xbar (nm)	Width (nm)	Xbara (nm)	Xbarv (nm)	S_Pt	Sp	Test ID	AMass ug/m3	EIn (No./kg)	EIm (g/kg)	AArea (um2/cm3)
00818b	1	1.970E+07	20.960	32.660	38.770	53.620	7	a	S218C1T1	3037.476	2.810E+16	3.403E+00	23260.2
	2	4.673E+07	22.260	33.630	40.470	55.890	8	b		8157.747	1.110E+17	1.523E+01	60106.8
	3	3.055E+07	22.880	34.860	41.840	57.740	9	a		5880.485	1.230E+17	1.863E+01	42000.6
	4	3.846E+07	24.480	34.600	43.550	59.080	10	a		7930.226	1.830E+17	2.964E+01	57283.6
	5	2.802E+07	21.560	32.400	39.250	53.970	12	a		4405.106	1.200E+17	1.476E+01	33905.3
	6	4.433E+07	26.940	37.320	47.520	64.260	13	a		11761.99	1.660E+17	3.459E+01	78614.2

Table B–1

yymddB	umr ID	Conc (No./cm^3)	Xbar (nm)	Width (nm)	Xbara (nm)	Xbarv (nm)	S_Pt	Sp	Test ID	AMass ug/m3	Eln (No./kg)	Elm (g/kg)	AArea (um2/cm3)
00822b	1	3.121E+07	19.110	32.730	36.200	51.840	1		S220C1T1	3414.475	7.735E+15	8.463E-01	32117.7
	2	1.470E+07	20.010	33.860	38.380	53.870	1			1804.883	4.363E+15	5.357E-01	17006.6
	3	2.230E+07	20.890	33.270	39.100	54.160	2			2782.727	4.855E+15	6.058E-01	26778.5
	4	1.983E+07	19.100	32.160	36.520	51.260	4			2097.306	3.662E+15	3.873E-01	20767.6
	5	1.579E+07	20.730	34.570	39.490	55.310	5			2098.645	2.853E+15	3.791E-01	19342.0
	6	6.558E+06	19.160	34.400	37.700	53.560	7			791.4143	1.962E+15	2.368E-01	7320.9
	7	1.710E+07	17.930	33.140	35.660	51.060	10			1788.157	3.364E+15	3.517E-01	17081.4
	8	2.261E+07	21.620	34.340	40.400	55.960	13			3111.48	4.460E+15	6.139E-01	28979.8
	9	1.541E+07	20.570	34.230	39.150	54.800	13		S220C1T2	1991.364	3.041E+15	3.931E-01	18546.9
	10	1.702E+07	19.340	32.620	36.940	51.960	12			1874.694	3.100E+15	3.416E-01	18235.4
	11	2.233E+07	19.870	33.260	37.880	53.140	10			2631.159	4.609E+15	5.432E-01	25159.4
	12	1.511E+07	22.230	35.420	41.530	57.650	8			2273.053	4.264E+15	6.417E-01	20461.3
	13	1.257E+07	20.570	33.810	38.900	54.380	7			1587.736	3.385E+15	4.275E-01	14940.3
	14	1.849E+07	20.810	35.880	40.080	56.690	7		S220C1T3	2645.168	4.951E+15	7.084E-01	23323.2
	15	2.634E+07	20.230	34.520	38.680	54.750	8			3395.408	6.248E+15	8.054E-01	30953.6
	16	2.844E+07	25.070	46.800	47.030	71.870	10			8290.621	5.163E+15	1.505E+00	49396.1
	17	2.396E+07	22.550	35.870	42.100	58.420	12			3751.683	4.209E+15	6.591E-01	33350.6
	18	2.078E+07	25.740	38.590	46.490	64.330	13			4344.873	3.701E+15	7.737E-01	35274.0
	19	2.011E+07	24.960	43.100	47.270	68.050	5						
00825b	1	3.133E+07	23.790	36.250	42.930	60.040	10	b	S221C1T2	5324.809	5.696E+15	9.682E-01	45342.2
	2	3.909E+07	28.710	37.990	50.230	66.700	2		S221C1T3	9109.164	7.198E+15	1.678E+00	77450.8
	3	2.686E+07	26.020	36.240	46.500	62.260	3			5090.679	4.227E+15	8.012E-01	45609.2
	4	3.545E+07	31.500	42.300	55.100	73.800	3	a		11190.56	6.275E+15	1.981E+00	84524.9
	5	2.840E+07	25.280	44.250	48.040	69.540	10	c		7500.635	4.602E+15	1.216E+00	51475.3
	6	2.416E+07	25.170	35.550	44.880	60.710	9	a		4246.064	3.968E+15	6.973E-01	38221.7
	7	2.729E+07	25.680	36.370	45.950	62.050	8	a		5120.775	4.618E+15	8.665E-01	45256.4
	8	2.757E+07	24.910	36.000	44.850	60.910	22			4892.851	4.521E+15	8.025E-01	43553.2
	9	3.177E+07	26.750	37.130	47.440	63.870	7	a		6501.689	5.142E+15	1.052E+00	56159.5
	10	3.446E+07	22.390	32.220	40.350	54.610	21			4407.552	5.951E+15	7.612E-01	44062.2
	11	3.523E+07	23.090	45.730	44.350	68.820	6	a		9019.287	8.346E+15	2.136E+00	54427.0
	12	1.805E+07	26.880	39.590	48.830	66.470	14			4163.371	3.586E+15	8.272E-01	33801.8
	13	1.360E+07	24.100	38.720	45.500	62.820	15			2647.645	2.682E+15	5.222E-01	22109.9
	14	1.522E+07	25.200	37.970	46.150	63.170	16			3014.063	3.049E+15	6.037E-01	25466.1
	15	1.925E+07	26.500	40.280	48.170	66.790	17			4504.363	3.805E+15	8.904E-01	35079.3
	16	1.880E+07	27.530	39.650	49.620	67.180	10	d		4476.096	3.253E+15	7.747E-01	36348.9

Table B–1 (Continued)

S	SO2 ppm	Pwr	Source Conc (No./cm^3)	Xbar (nm)	dera2000 S.wb3 Width (nm)	Xbara (nm)	Xbarv (nm)	AMass (ug/m^3)	Eln	Elm	AArea (um2/cm3)
L	830	Cr	1.648E+07	20.516	33.868	38.880	54.386	2.072E+03	3.68E+15	4.69E-01	1.947E+04
H	2300	Cr	1.876E+07	19.819	33.559	37.931	53.378	2.236E+03	4.16E+15	4.95E-01	2.117E+04
L	550	UpC	2.666E+07	25.844	38.515	46.806	64.359	5.701E+03	4.81E+15	1.04E+00	4.618E+04
H	2350	UpC	2.302E+07	23.227	39.127	43.608	62.352	4.486E+03	4.85E+15	8.90E-01	3.446E+04

Changes in aerosol parameters with changes in fuel sulfur content:

Slope	Cr	1549.1	-0.0005	-2E-04	-0.000645408	-0.000686	0.1119286	3.24E+11	1.71E-05	1.160303403
F.Change(LS-HS)		0.13	-0.03	-0.01	-0.02	-0.02	0.08	0.12	0.05	0.08
Slope	UpC	-2021.7	-0.0015	0.0003	-0.001776273	-0.001115	-0.6750275	2.6E+10	-8.1E-05	-6.51168121
F.Change(LS-HS)		-0.15	-0.11	0.02	-0.07	-0.03	-0.24	0.01	-0.15	-0.29

Changes in aerosol parameters with changes in power setting:

F.Change	LS	0.47	0.23	0.13	0.18	0.17	0.93	0.27	0.75	0.81
F.Change(Cr-UpC)										
F.Change	HS	0.20	0.16	0.15	0.14	0.16	0.67	0.15	0.57	0.48
F.Change(Cr-UpC)										

The aerosol parameters shown here (Source Conc, xbar, width,...) are averages for all probe positions for fixed sulfur content and power setting.

Table B–2

	AMass	Ein	Eim	Aarea
8/18 Uprated Cruise	.90	.31	.73	.88
8/22 Cruise	.56	.46	.44	.61
8/22 Uprated Cruise	.44	.57	.58	.53
8/25 Uprated Cruise	.69	.68	.79	.80

Table B–3

C Appendix—Aerodyne Emissions Measurements

Jody Wormhoudt and Rick Miake-Lye
Aerodyne Research, Inc.
45 Manning Road
Billerica, Massachusetts 01821–3976

C.1 Introduction

Aerodyne Research performed infrared absorption measurements of gas sampled from the combustor, using infrared tunable diode lasers and a multipass cell operating at reduced pressure. The apparatus used allowed simultaneous measurements by two lasers operating in two separate spectral regions. However, to get both good spectral resolution and the fast scanning which suppresses noise, only one laser was operated at a time. One laser was devoted to measuring SO_x species, both the relatively stable SO_2 and the highly reactive SO_3. At different times, the SO_x laser was operated in two spectral regions within the range of 1382 to 1383 cm^{-1}, containing a number of strong SO_2 lines, and also in a region from 1401 to 1402 cm^{-1}, having one of the best ratios of SO_3 to SO_2 line strengths.

Another reactive species, HONO, was the target of the second laser diode. Here again, two spectral regions were used at almost every test point, both in the 1666 to 1667 cm^{-1} range. Each of the five spectral regions also contained absorption lines of water vapor, so that emission index values for SO_2, SO_3, and HONO can be derived directly from our observations of concentrations of both the trace species and the water vapor. The use of multiple spectral regions was important in that it allowed estimation of the accuracy of our SO_2, HONO and water concentration measurements directly from our observations.

C.2 Apparatus Overview

For a given diode, the range of spectral regions which may be selected by changing diode temperatures is typically limited to at most 100 cm^{-1}. This can be done without physical access to the instrument, and typically only requires a few minutes equilibration time. Access to still other spectral regions can be obtained by physically changing the position of the collection optics in front of the laser dewar. Each side of the laser dewar holds up to four laser diodes. Other diodes available for this test were capable of measuring NO, NO_2, and CO_2. A CO_2 measurement, carried out in a spectral region above 2200 cm^{-1}, is particularly useful in resolving questions about the accuracy of emission indices derived using water concentration measurements. Questions can arise because in order to use water concentrations as a measure of fuel-to-air ratio in the exhaust, one must subtract the water level due to humidity in the inlet air. However, changing from one diode to another requires physical access to the instrument and up to a half hour of alignment and equilibration time, so only the SO_x and HONO diodes were operated in the present test.

The main components of the Aerodyne infrared tunable diode laser apparatus used in this test were: an optical table containing lasers, a multipass cell, and infrared detectors; an electronics rack containing diode controllers and the data acquisition computer; and a mechanical pump to draw the exhaust sample through the multipass cell. If the instrument is to be left unattended for more than 8 hours, it can be connected to a liquid nitrogen tank and autofill system; in this

test, the liquid nitrogen dewar which contained both the laser diodes and infrared detectors was periodically refilled by hand. A long cable to a second monitor and keyboard allowed remote operation of the apparatus.

The most serious hardware problems we faced were fouling of the multipass mirrors by combustor soot, and an intermittent dramatic increase in modulation of the diode intensity (the latter resembled the effects expected from vibration but could not be traced to a particular source in the test cell). Both problems were surmounted, the former by dismantling the multipass cell between test days and cleaning the mirrors, the latter by using averaging periods of 30s or more.

C.3 Trace Species Sampling

The sampling probe was designed to allow measurement of reactive species, within the constraints of also providing sample gas streams to the conventional gas analysis instruments operated by DERA and the particle measurement system operated by UMR. The probe assembly involved a short, large diameter water-cooled section (39.3 cm length, 0.8 cm id) operating at the combustor pressure, followed by a "splitter" block in which the sampled gas was divided into three streams. Here, the TDL sample passed through a small (0.03 cm diameter) orifice of finite length (0.1 cm). This orifice resulted in a pressure drop from the 7 or 8 atm combustor pressures to the 25–35 Torr multipass cell pressures. The low pressure gas sample passed from the orifice through another short (20 cm) length of stainless steel tubing and then through a 1.5 m length of 0.5 in (0.955 cm id) PFA tubing. The PFA tubing was swaged onto the stainless tubing stub of the probe, and passed into the multipass cell through an O-ring seal coupling.

The tubing section of the probe downstream of the orifice in the splitter block also contained provisions for the introduction of a flow of dilution gas. Our main motivation was to give us some additional control on the sample gas temperature, to prevent overheating the multipass cell. (Because of the drop in pressure through the small orifice, sample dilution to prevent water condensation was not necessary.) It turned out that the sample gas had already cooled substantially before passing through the orifice in the splitter block. The dilution gas was also introduced in such a way that it could to some extent form a shield flow, to minimize contact between the sample gas and the walls of the probe. We used tank nitrogen as the dilution gas, and the flow was monitored by a rotameter.

Because we ratio trace gas concentrations to water concentrations to obtain emission indices, and because only part of the water in the exhaust sample was derived from the fuel, we need to know the ratio of dilution gas to exhaust sample gas. We had originally intended to compute this from absolute values of the flow through the sampling orifice and the dilution gas flowmeter. However, because of the position of the valve included with the dilution nitrogen rotameter, the pressure in the rotameter tube did not remain constant but varied with the flow rate, meaning that accurate values of the dilution flow were not directly measured. As it turns out, cell pressure readings were taken both with sample gas and dilution gas flows alone, as well as with the combined flows used during measurements. Therefore, with a *post facto* calibration we could deduce the individual flows through the sampling orifice and the dilution nitrogen flowmeter, and so the ratio of sample flow to total flow we desire. However, as we examined the data points available to us, we came to the conclusion that a more accurate way of determining the dilution ratio was to compare our TDL measurements of water concentrations in the our diluted sample with the water concentrations in the undiluted sample reported by DERA.

The latter values are not directly measured, but derived from CO_2 measurements, inlet humidity measurements, and the C/H ratio of the fuel. However, we found there was a good correlation between the two sets of water concentrations, which gave consistent values of dilution ratios for the same nitrogen flowmeter settings. At various times in our measurements we used dilution flowmeter readings of "5 slpm" or "10 slpm" (because the rotameter tube pressures were below 1 atmosphere, the true flow rates were lower). These two dilution gas settings corresponded to dilution ratios (total flow to sample flow) of 1.4 and 2.1 respectively, as determined by comparing water concentrations.

C.4 SO_3 Region Observations

A major focus of our work, the measurement of the reactive species SO_3, unfortunately yielded no positive results, and thus can be dealt with briefly in this report. While we had originally intended to measure SO_2 and SO_3 in the same spectral region (one of the 1382 cm^{-1} regions) it soon became clear that the SO_2/SO_3 was much too large for this to work well. The 1401 cm^{-1} spectral region, where the ratio of SO_3 to SO_2 line strengths is greatest, was observed throughout the tests, but we need only focus on the two brief periods when very large sulfur doping levels were used, early in the 8/22 and 8/25 test days. Analysis of these spectra during the field test was hampered in the following ways: 1) this spectral region was not our first choice for SO_3 measurement, but instead was the best available allowed by the diode operating characteristics after shipping; 2) as a result, pre-test calibration spectra were not available for either SO_2 or SO_3, as they were for our first-choice spectral regions; 3) the HITRAN line listing of SO_2 line positions only extends to 1400 cm^{-1}; and, 4) our model of the SO_3 spectrum, constructed from line positions in the literature from a laboratory study, and first-principles intensities, turned out to have a flaw in the relative intensities assigned to one of the many bands. The result of all these developments was that it was not immediately obvious whether the lines observed at 1401 cm^{-1} during the two high sulfur periods were due to SO_3 or SO_2.

After we returned from DERA, we were able to operate the TDL instrument in our laboratory to take spectra of both SO_3 and SO_2 in this spectral region. We were additionally able to match up our SO_3 spectral model with the observed spectra and determine the error in our model intensities (although as yet the reason for this discrepancy is not clear). Finally, we were also able to obtain a new SO_2 line list in the 1401 cm^{-1} region from the spectroscopists who are developing a revision to the HITRAN listing. With all of this additional information, the identity of the spectra we observed at DERA is clear: only SO_2, not SO_3, was observed even at the high sulfur loadings.

We used SO_2 spectra obtained in our laboratory after the field test to subtract out the SO_2 features in our DERA exhaust gas spectra, then examined the resulting residual spectra to estimate an upper limit SO_3 concentration. Our estimate is that the ratio of SO_3 to SO_2 concentrations in our multipass cell was less than 10^{-3}. Going beyond this, to an estimate of the fraction of sulfur in the form of SO_3 in the combustor, requires an estimate of the fraction of SO_3 that is lost in the sampling line. If 90 percent is lost, the upper limit for SO_3 in the combustor would be 1 percent, while if 99 percent were lost in the sampling line, the upper limit for SO_3 in the combustor would be 10 percent of the combined sulfur species.

C.5 SO_2 and HONO Observations

We now turn to the observations of SO_2 and HONO, species whose spectra we were indeed able to observe and quantify. Figures 1 through 6 show examples of observed spectra in the

two spectral regions used for each of the two species. It can be seen in Figures 1 and 2 that SO_2 lines are easily observed in both regions, and that these regions differ primarily in the positions of water lines. Both the degree of overlap between water and SO_2 lines, and the position of the strong water line in Figure 1 at the left of the scan, where the laser tuning rate is fastest, can affect the quality of the data, especially the quality of the water concentrations. That said, except at the very high sulfur loadings there was very good agreement between sulfur emission indices determined from the two spectral regions.

The situation is different for HONO since, as can be seen in Figures 3 through 6, the HONO concentrations we observed are only slightly above our detection limit for this particular diode and spectral region. These spectra were all taken during the same engine condition/probe position data point, and illustrate a consistent property of the HONO data set: one spectral region consistently yields HONO concentrations that are up to double those determined from the other spectral region. This occurs because the least squares fit is sensitive to small, systematic residual differences in the shapes of the baselines in the two regions. By contrast, the water concentrations yielded by the two spectral regions are almost identical, since the water lines are so much stronger than the noise level in the baseline. Unfortunately, given the noise level in the spectra, it is not possible to determine which spectral region's automated analysis is closer to the truth. Our best estimate, after examining a number of spectra, is that the true HONO concentration lies between the values yielded by the least squares fitting of the two regions. As a result, we adopted the following rule for automated analysis of the HONO spectra: we accepted the results of least squares fits to all spectral regions, even if they appeared to underestimate or overestimate HONO concentrations, then averaged the concentrations from both regions. This procedure is also followed for SO_2, although there the values being averaged are typically much closer to each other. Water concentrations from all spectral regions are also averaged to provide a single best estimate of water concentration in the multipass cell. Values of all these concentrations are reported in Tables 1 and 2 for the two days in which we observed sulfur doping runs.

Also reported in Tables 1 and 2 are values of water concentrations in our multipass cell which are derived from humidity in the inlet air. These concentrations are derived from DERA measurements of inlet air humidity, and the sample dilution ratios discussed above. These water concentrations are subtracted from the total water concentrations in the adjacent column to yield concentrations of water derived from the fuel. It is this latter concentration which is divided into the trace gas concentration (and multiplied by a scaling factor) to yield an emission index. In the case of HONO the emission indices are reported, while for SO_2 an additional conversion is made so that instead of emission index (weight of SO_2/1000X weight of fuel) the fraction of sulfur (in the measured SO_2) in the fuel is reported. This can be compared directly with laboratory analyses of fuel sulfur carried out on fuel samples drawn by DERA during the test. These values are also recorded in Tables 1 and 2.

The comparison between TDL SO_2 measurements and laboratory analyses is also shown in Figure 7. The example error bar shown in this figure is derived from two sources: an estimate of precision derived from an average 12 percent standard deviation observed in repeated measurements of SO_2 emission indices under the same conditions, and an estimate of systematic uncertainties (including error limits in molecular band strengths, for example) of 16 percent. Adding these two estimates in quadrature results in the 20 percent uncertainty limit shown in the figure. It can be seen that most TDL measurements agree with the corresponding laboratory analysis point to within this uncertainty limit. An exception is the first of two laboratory analyses of the low sulfur fuel used for most of the 8/25 test. The reason for this

discrepancy is not clear. Our overall conclusion is that the TDL measurements show that the great majority of the fuel sulfur was in the form of SO_2 in the exhaust, and that the uncertainties in both the SO_2 and fuel sulfur measurements preclude any estimates of concentrations of other species, such as SO_3, by differencing the SO_2 and total sulfur values.

The 30 values of HONO emission index reported in Tables 1 and 2 have a mean of 0.026, and a percentage variance (100 x variance/mean) of 26 percent. By comparison, the average of the same 30 values of NO emission index as reported by DERA is 8.3, and its variance is 11 percent. If we first ratio HONO EI to NO EI at each point, then average the ratios, that average value is 0.0033. The variance in this set of ratios is 33 percent. This is only slightly smaller than the expected variance if the two EI arrays were uncorrelated, that is, the variance obtained by adding 26 percent and 11 percent in quadrature to obtain 35 percent. This means that the evidence for a significant correlation between NO and HONO concentrations is small, but it also means that there is no evidence that they are anti-correlated. The small fraction of HONO compared to NO is expected. Indeed, the remaining question is whether the observed HONO concentrations are too large to be due only to HONO formed in the combustor, or whether formation in the probe also contributes.

Finally, we want to consider further whether the array of HONO emission indices carries any additional information beyond the average value discussed above. In order to investigate the possibility of systematic, steady-state differences in HONO concentration with position in the combustor, we averaged all available HONO emission indices for each probe position, separating values only between uprated cruise and normal cruise combustor conditions. To do this, we drew on two additional HONO data sets. One was obtained early in the 8/25 test day, when undoped fuel was used to quickly re-do a set of DERA gas-sampling observations. Rather than collect spectra for all species, we kept the TDL on one HONO region and wrote a continuous record (a so-called “streaming file”) of HONO and water concentrations, which could later be analyzed and averaged to yield HONO emission indices for several probe positions. The second added data set was obtained for several points during the 8/18 test day, also using undoped fuel. We saw no systematic differences between these two additional data sets and the data sets reported in Tables 1 and 2.

The array of possible probe positions is essentially laid out in three horizontal rows. However, only two of our observations were derived from probe positions in the bottom row. Therefore, in Figures 8 and 9, only data from the middle and top rows are depicted. As discussed above, the spread in values of HONO concentrations is much larger than is the case for SO_2, both between the two spectral regions and within the data set associated with one spectral region. When we carry out the same error-estimation procedures as outlined above for SO_2, the precision estimate derived from standard deviations is much larger, so that the overall estimate of an uncertainty limit rises from 20 to 48 percent. This uncertainty limit is plotted in Figures 8 and 9. As discussed above, the high noise levels involved in individual HONO observations mean higher variances at every step of the analysis. Some bars in Figures 8 and 9 are based on a single measurement set. However, averaging two or three values is observed to cause a speedy regression to the mean. Furthermore, in the case of the central spatial point (point 10 in the identification scheme used during the test, numbered 6 in Figures 8 and 9) for the uprated cruise condition, the five values we measured over the three days had a variance of less than 20 percent.

In general, we cannot say that any significant spatial variation is seen in Figures 8 and 9. However, we can point out that the left-hand side of Figure 9 is based in large part on the

real-time observations of the 8/25 no-doping data set, and reproduces the trend seen in that data set alone, of an increase in HONO moving from the wall to the center of the combustor. These observations, of differences in HONO at five spatial points accessed over 30 minutes, are more likely to bring out systematic trends than are averages over data points collected over several days.

C.6 Summary

Tunable diode lasers were used to measure concentrations of SO_2, SO_3, HONO and water vapor in sampled combustor gas. SO_3 concentrations, after whatever probe losses occurred during these tests, were below our detection limit, and our best estimates to date are consistent with an upper limit on fraction of sulfur in the form of SO_3 in the combustor of at most a few percent. Comparison of our measurements of SO_2 emission index with fuel analyses for total sulfur yield the same conclusion, that the great majority of sulfur was in the form of SO_2 in the combustor exhaust. Our observed HONO concentrations were a small fraction of total NO_x emissions, although they may be large enough to raise questions of whether some HONO was formed in the sampling process.

In general, the TDL instrument operated well throughout the tests. Collection of data in multiple spectral regions proved to be a very useful diagnostic of measurement accuracy. Use of water concentrations as the reference for emission index determination, with the associated requirements to quantify the dilution factor and the inlet air humidity, added several issues to the data analysis task, but on the whole these issues seem to have been well enough resolved that the data set is now well understood.

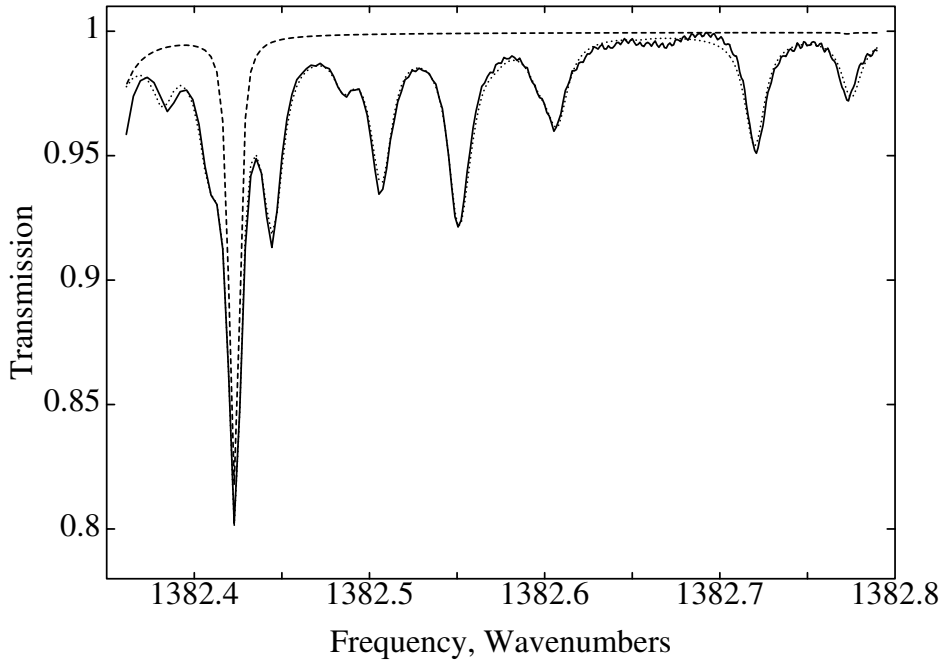

Figure 1 – Spectrum of First SO_x Region: Observed Spectrum (Solid Line), Model Fit (Dotted Line) and Model with Water Lines Only (Dashed Line).

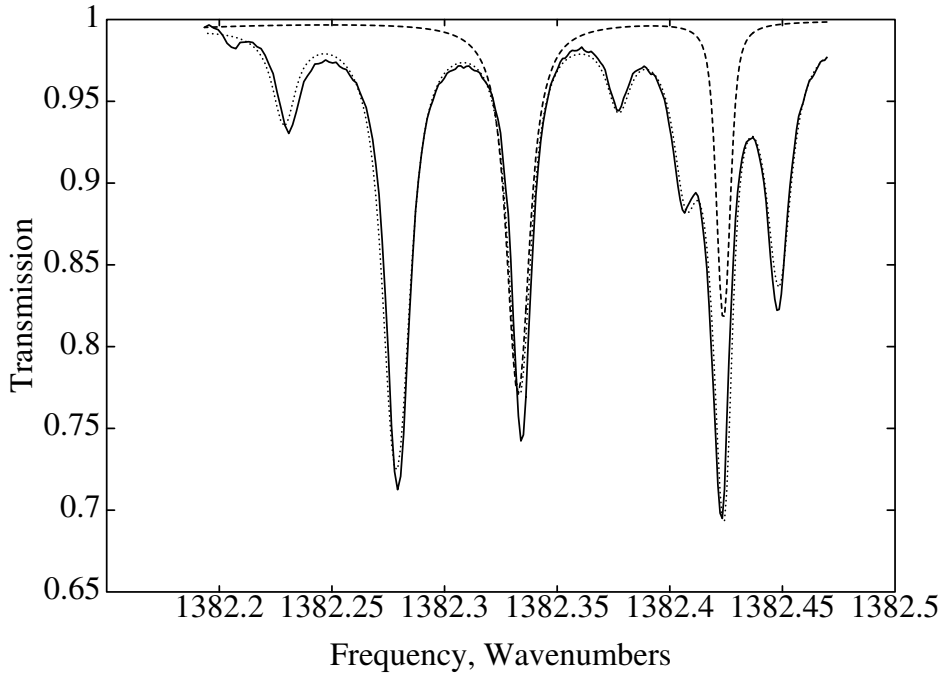

Figure 2 – Spectrum of Second SO_x Region: Observed Spectrum (Solid Line), Model Fit (Dotted Line) and Model with Water Lines Only (Dashed Line).

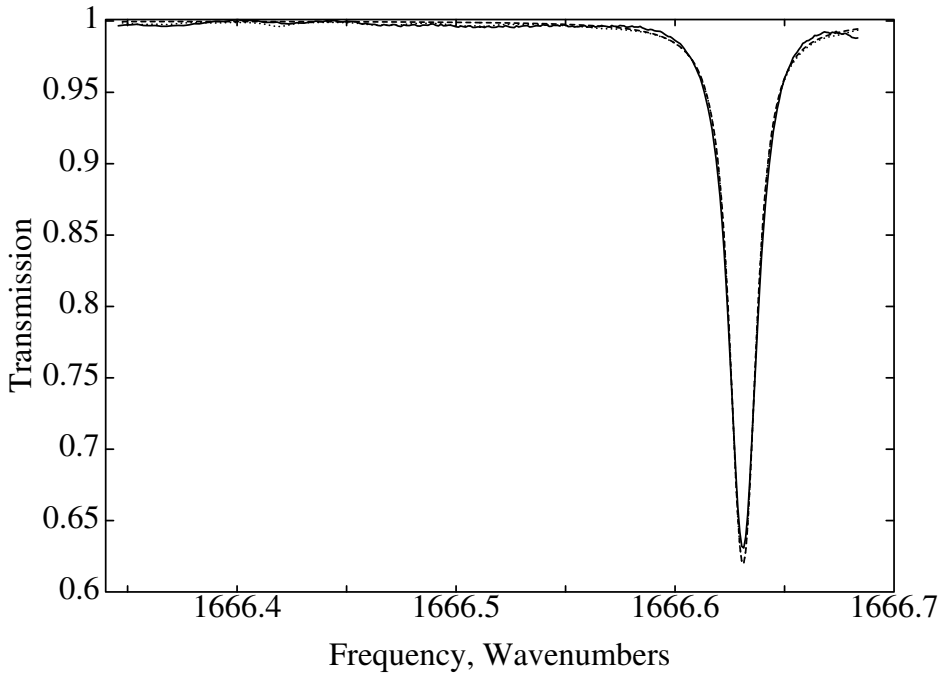

Figure 3 – Spectrum of First HONO Region: Observed Spectrum (Solid Line), Model Fit (Dotted Line) and Model with Water Lines Only (Dashed Line).

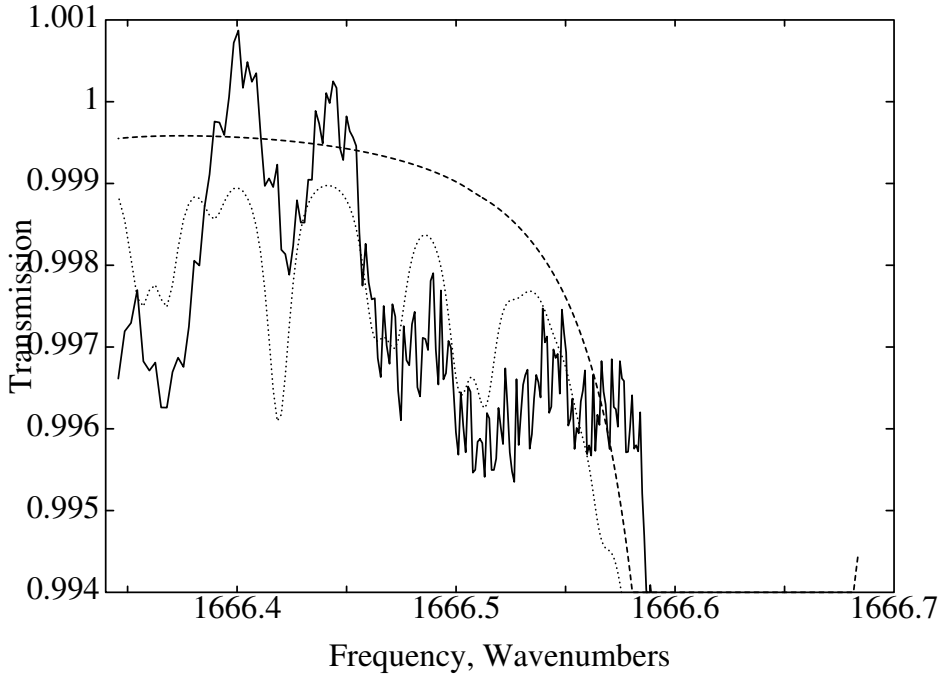

Figure 4 – Spectrum of First HONO Region, with Scale Expanded to Show HONO Lines (Model Fit for 220 ppbv HONO in Multipass Cell).

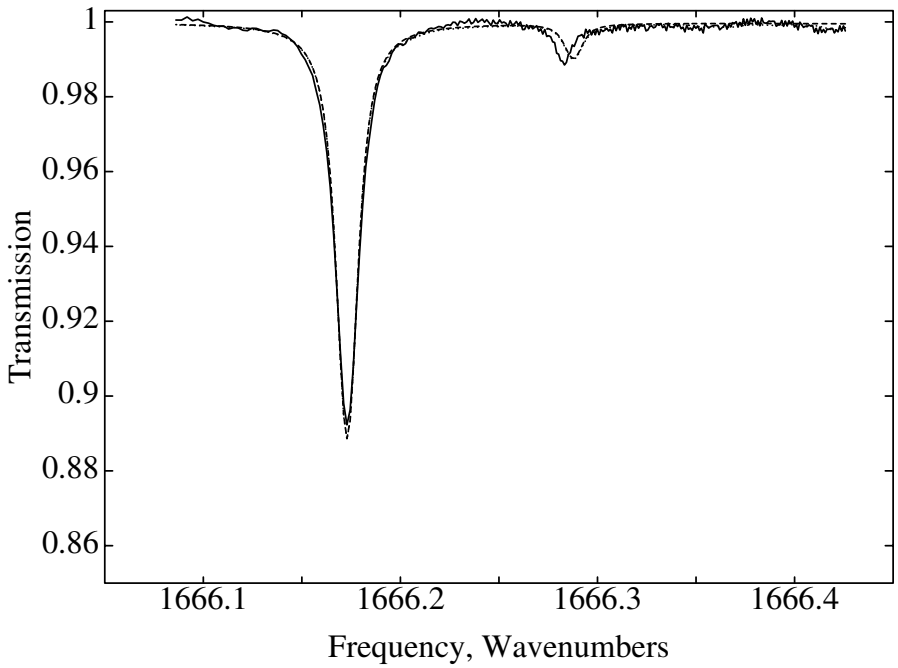

Figure 5 – Spectrum of Second HONO Region: Observed Spectrum (Solid Line), Model Fit (Dotted Line) and Model with Water Lines Only (Dashed Line).

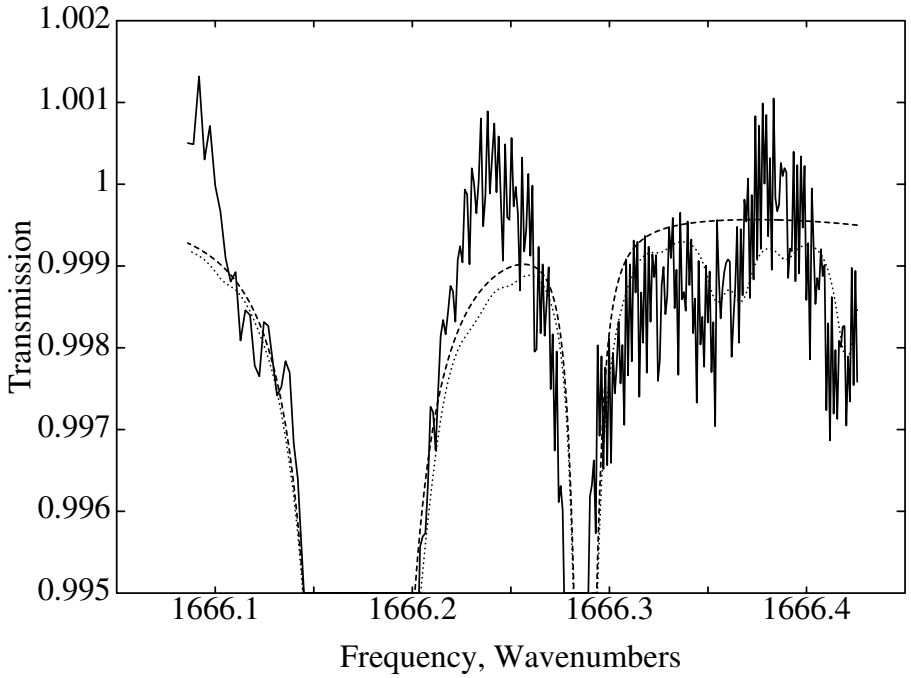

Figure 6 – Spectrum of Second HONO Region, with Scale Expanded to Show HONO Lines (Model Fit for 105 ppbv HONO in Multipass Cell).

Table 1 – Summary of TDL Results for 8/22/00 Data Set.

Spatial Point	Start Time/ End Time		SO_2, ppm_v in Cell	Fuel S, ppm_{wt}	Fuel S, Analysis	HONO ppb_v in Cell	HONO EI (as NO_2)	H_2O in Cell	Humidity H_2O Subtracted
Uprated Cruise									
10	9:43	9:44	95	5500	11650[a]			4.27	0.51
1	9:54	10:09	52	8300		120	0.028	1.88	0.51
1	10:24	10:37	8.2	1620	1600	58	0.016	1.67	0.56
Normal Cruise									
1	10:55	11:07	7.9	2270	2300	98	0.040	1.37	0.61
2	11:15	11:28	12	1870		155	0.035	2.01	0.61
4	11:30	11:44	16	1850		152	0.025	2.50	0.61
5	11:51	11:59	16.5	1820		210	0.033	2.60	0.61
7	12:09	12:21	7.8	2250		96	0.040	1.41	0.65
10	12:27	12:34	13.8	1820		136	0.026	2.31	0.65
13	12:45	13:01	12.6	1690		124	0.024	2.24	0.61
13	13:16	13:36	5.5	785	830[b]	172	0.035	2.18	0.65
12	13:40	13:54	7.4	920		137	0.024	2.41	0.65
10	13:58	14:06	4.0	620		128	0.028	2.07	0.65
10	14:07	14:13	8.4	845				3.18	1.00
8	14:14	14:27	5.8	900		168	0.037	2.48	1.07
7	14:31	14:40	4.4	800		109	0.029	2.27	1.07
Uprated Cruise									
7	15:15	15:28	22	3680	2350[c]	120	0.029	2.45	1.14
8	15:31	15:45	27	3440		107	0.020	2.86	1.14
10	15:48	16:00	43	3170		207	0.022	4.18	1.21
12	16:03	16:15	45	2900		183	0.017	4.60	1.21
13	16:21	16:32	43	2880		143	0.014	4.48	1.21
5	16:38	16:55	12	890		203	0.022	4.16	1.21

[a] Fuel sample taken at 10:10, presumed to apply to doping level from 9:43 on.
[b] Fuel sample taken at 14:05, presumed to apply to doping level from 13:16 on.
[c] Fuel sample taken at 16:45, presumed to apply to doping level from 15:15 on.

Table 2 – Summary of TDL Results for 8/25/00 Data Set, Sulfur Doping Points.
All Points Are for Uprated Cruise Combustor Condition.

Spatial Point	Start Time/ End Time		SO_2, ppm_v in Cell	Fuel S, ppm_{wt}	Fuel S, Analysis	HONO ppb_v in Cell	HONO EI (as NO_2)	H_2O in Cell	Humidity H_2O Subtracted
10	11:19	11:21	117	8960	7500			3.79	0.93
10	11:40	11:49	5.8	390	550[a]	237	0.023	4.19	0.93
2	11:51	12:03	4.7	320		183	0.018	4.17	0.93
3	12:05	12:38	4.7	270		353	0.029	4.77	0.93
10	12:52	13:03	6.5	365		336	0.027	4.89	1.00
9	13:06	13:17	6.3	355		386	0.031	4.97	1.07
8	13:21	13:33	5.6	325		229	0.019	4.84	1.07
22	13:37	13:48	5.9	330		281	0.023	4.92	1.00
7	13:53	14:05	6.6	370		288	0.023	4.94	1.00
21	14:06	14:18	5.4	340				4.50	1.00
6	14:19	14:35	3.6	300				3.64	1.00
14	14:36	14:48	3.9	310		224	0.025	3.79	1.00
15	14:49	14:57	4.0	290				4.00	1.00
16	15:01	15:13	4.4	340		240	0.026	3.85	1.00
17	15:15	15:28	4.6	380				3.73	1.07
10	15:29	15:39	5.6	370	400			4.40	1.07
22	15:40	15:45	5.4	365				4.32	1.07

[a] Fuel sample taken at 12:15, presumed to apply to doping level from 11:40 on.

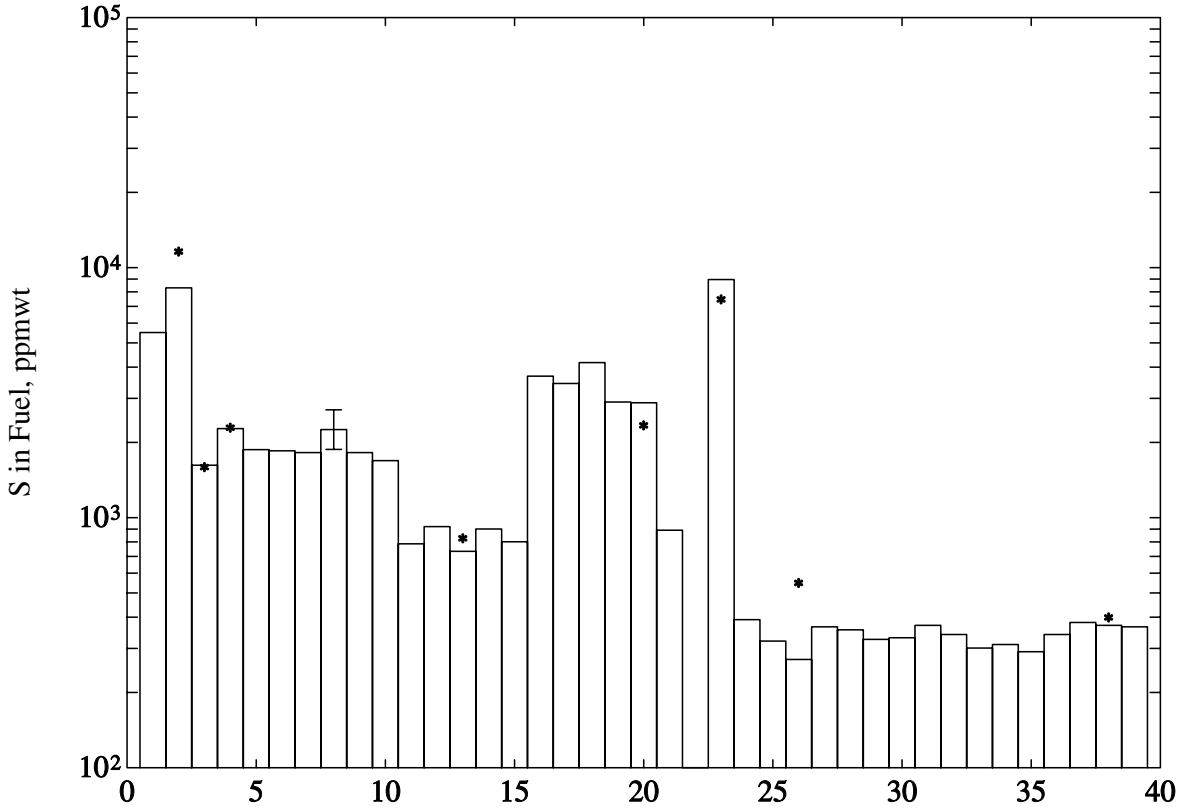

Figure 7 – TDL Measured SO_2 Expressed as Weight of Sulfur in Fuel, for 8/22/2000 and 8/25/2000 Data Sets. The Stars Denote DERA Fuel Analyses. The Error Bar Is an Example of the 20 Percent Accuracy Estimate Assumed for All Measurements. (The Precision Estimate Derived from Standard Deviations of Repeated Measurements Was 6 Percent.)

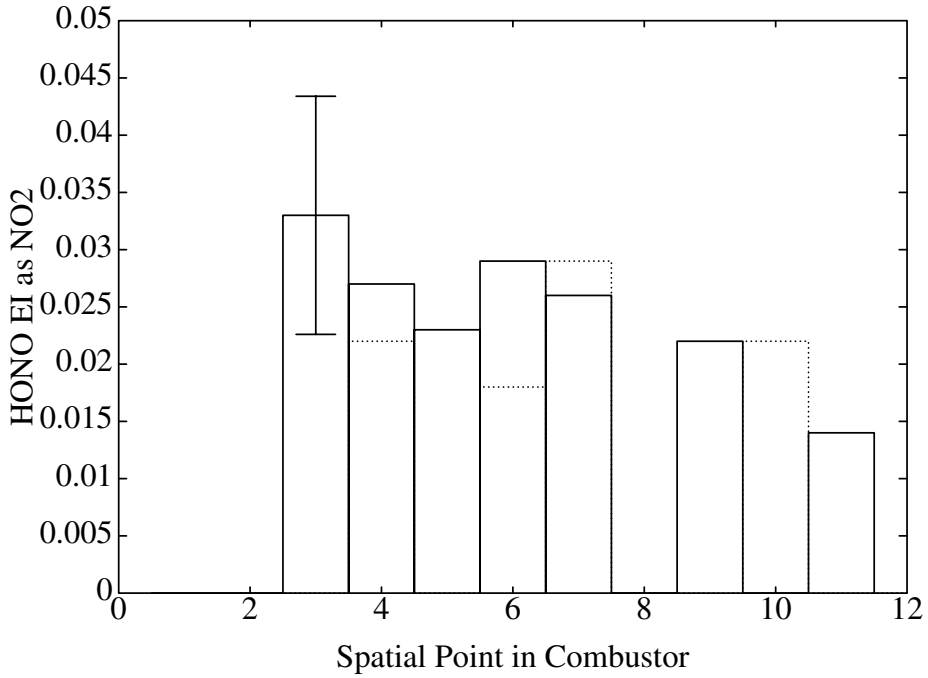

Figure 8 – HONO Emission Index for Uprated Cruise Conditions (Averages of All Values Observed on 8/18, 8/22 and 8/25/00. Middle Row (Solid) and Top Row (Dots).

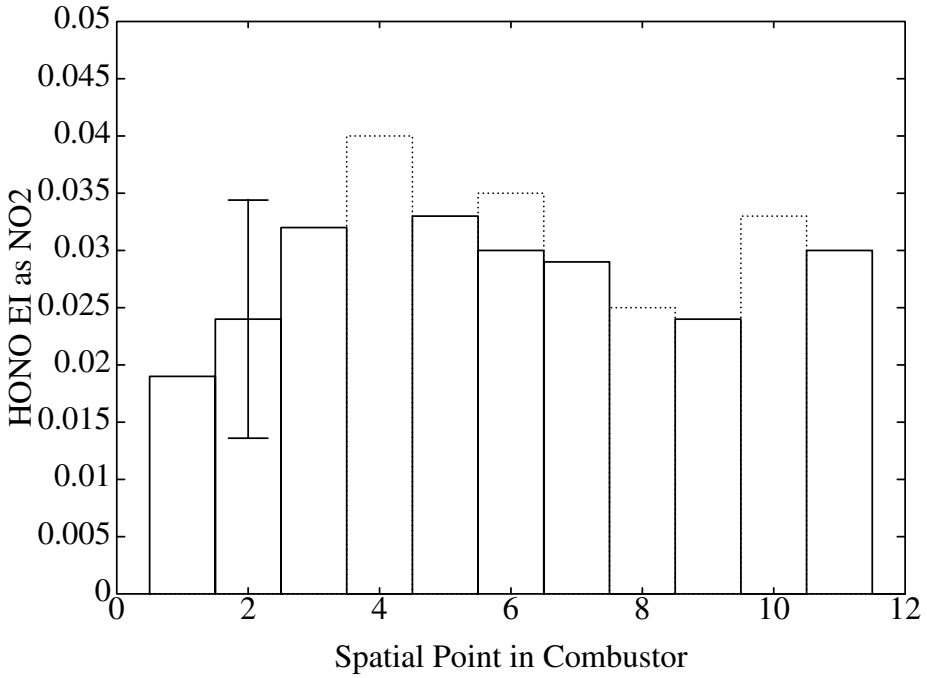

Figure 9 – HONO Emission Index for Normal Cruise Conditions (Averages of All Values Observed on 8/18, 8/22 and 8/25/00. Middle Row (Solid) and Top Row (Dots). (See Text for Discussion of Error Bars.)

REPORT DOCUMENTATION PAGE

Form Approved
OMB No. 0704-0188

1. AGENCY USE ONLY (*Leave blank*)	2. REPORT DATE	3. REPORT TYPE AND DATES COVERED
	September 2002	Final Contractor Report

4. TITLE AND SUBTITLE

NASA/DERA Collaborative Program—Interim Report

5. FUNDING NUMBERS

WU–714–01–20–00
NAS3–98102, NAG3–2179,
NAG3–2185
1L162211A47A

6. AUTHOR(S)

Phillip D. Whitefield, Donald E. Hagen, Jody C. Wormhoudt,
Richard C. Miake-Lye, Kevin Brundish, and Christopher W. Wilson

7. PERFORMING ORGANIZATION NAME(S) AND ADDRESS(ES)

University of Missouri at Rolla
Rolla, Missouri 65401

8. PERFORMING ORGANIZATION REPORT NUMBER

E–13586

9. SPONSORING/MONITORING AGENCY NAME(S) AND ADDRESS(ES)

National Aeronautics and Space Administration
Washington, DC 20546–0001
and
U.S. Army Research Laboratory
Adelphi, Maryland 20783–1145

10. SPONSORING/MONITORING AGENCY REPORT NUMBER

NASA CR—2002-211899
ARL–CR–0509

11. SUPPLEMENTARY NOTES

Phillip D. Whitefield and Donald E. Hagen, University of Missouri at Rolla, Rolla, Missouri; Jody C. Wormhoudt and Richard C. Miake-Lye, Aerodyne Research, Inc., Billerica, Massachusetts; and Kevin Brundish and Christopher W. Wilson, Defence Evaluation and Research Agency, Farnborough, Hampshire, England. This Document was produced by QinetiQ for The Department of Trade and Industry Under Order/Contract reference F11X1DXX. Copying and use of the document is restricted to that set out in the referenced Order/Contract and the document may not otherwise be used or disseminated without written consent of QinetiQ. Approval for wider use of releases must be sought from: Intellectual Property Department, QinetiQ ltd, Cody Technology Park, Farnborough, Hampshire GU14 0LX. Project Manager, Chowen C. Wey, Vehicle Technology Directorate, NASA Glenn Research Center, organization code 0300, 216–433–8357.

12a. DISTRIBUTION/AVAILABILITY STATEMENT

Unclassified - Unlimited
Subject Categories: 01, 07 and 09 Distribution: Nonstandard

Available electronically at http://gltrs.grc.nasa.gov

This publication is available from the NASA Center for AeroSpace Information, 301–621–0390.

12b. DISTRIBUTION CODE

13. ABSTRACT ***(Maximum 200 words)***

This report is an interim report of the work reported are the results from the combustor testing, the first phase of testing in the DERA/NASA collaborative program. A program of work was developed by DERA and NASA utilizing specialist facilities within the UK, and specialist measurement techniques developed within the U.S. Under a Memorandum of Understanding (MoU) between the UK and U.S. governments, the joint UK/U.S. funded program commenced. The objective of the program was to make combustor and engine exit plane emissions measurements, including particulate and sulphur measurements, for kerosene fuels with different sulphur levels. The combustor test program was performed in August/September 2000. Although probe issues complicated the test program, a consistent set of data, including CO, NO_x, NO, NO_2, CO_2, O_2, smoke number, particulate number density and size distribution, SO_2, SO_3 and HONO were collected at the exit plane of the DERA TRACE engine combustor. A second probe was utilized to measure spatial location of CO, NO_x, NO, NO_2 and CO_2 concentrations. Data are therefore available for development of aerosol, particulate and aerosol precursor chemistry sub-models for inclusion into CFD. Inlet boundary conditions have been derived at the exit of the combustion system for the modelling of the DERA TRACE engine. The second phase of the program is to perform identical measurements at the engine exit, to allow a full data set to be available. This will be performed in July 2001 at the Glenn test facility, DERA Pyestock.

14. SUBJECT TERMS

Combustor emissions measurement; Particulate emissions; Turbine trace chemistry modeling

15. NUMBER OF PAGES

81

16. PRICE CODE

17. SECURITY CLASSIFICATION OF REPORT	18. SECURITY CLASSIFICATION OF THIS PAGE	19. SECURITY CLASSIFICATION OF ABSTRACT	20. LIMITATION OF ABSTRACT
Unclassified	Unclassified	Unclassified	